

AD-A022 433

LIFT, DRAG, AND PRESSURE DISTRIBUTION EFFECTS
ACCOMPANYING DRAG-REDUCING POLYMER INJECTION ON
TWO-DIMENSIONAL HYDROFOIL

Daniel H. Fruman, et al

Hydronautics, Incorporated

Prepared for:

Office of Naval Research

October 1975

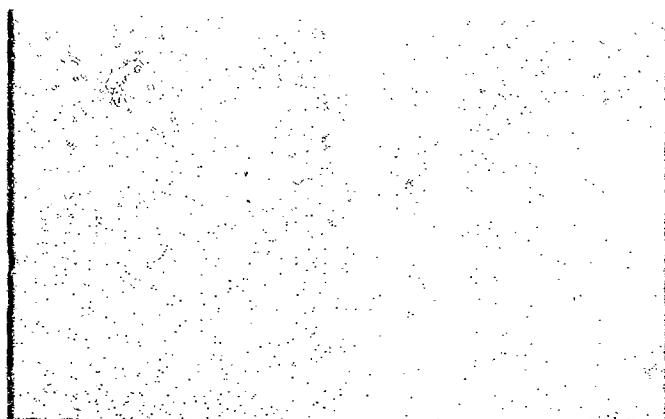
DISTRIBUTED BY

NTIS

National Technical Information Service
U. S. DEPARTMENT OF COMMERCE

093103

ADA022433



Approved for public release; distribution unlimited.

CO
CONFIDENTIAL
A

HYDRONAUTICS, incorporated research in hydrodynamics

Research, consulting, and advanced engineering in the fields of NAVAL
and INDUSTRIAL HYDRODYNAMICS. Offices and Laboratory in the
Washington, D. C. area: Pinball School Road, Howard County, Laurel, Md

SP-000007-2 BY
NATIONAL TECHNICAL
INFORMATION SERVICE

HYDRONAUTICS, Incorporated

TECHNICAL REPORT 7101-5

LIFT, DRAG, AND PRESSURE
DISTRIBUTION EFFECTS ACCOMPANYING
DRAG-REDUCING POLYMER INJECTION
ON TWO-DIMENSIONAL HYDROFOIL

By

D. H. Fruman,
Marshall P. Tulin,
and Han-Lieh Liu

October 1975

Approved for public release; distribution unlimited.

Prepared for
Office of Naval Research
Department of the Navy
Under
Contract No. N00014-71-C-0063
NR 062-325

RECEIVED
A

SECURITY CLASSIFICATION OF THIS PAGE (When Data Entered)

DD FORM 1 JAN 73 1473

UNCLASSIFIED

SECURITY CLASSIFICATION OF THIS PAGE (When Data Entered)

UNCLASSIFIED

SECURITY CLASSIFICATION OF THIS PAGE(When Data Entered)

20. Cont'd.

slits were situated at 10 and 30 percent of the chord length.

The pressure distribution data does not indicate any significant change of the separation point. It demonstrates, however, that the polymer injection always results in a significant decrease of pressure in the region aft of the injection slit.

This decrease of the local pressure gives rise to a lift increase for injections made on the suction side of the foil surface and a lift decrease for injections made on the pressure side.

The data suggest an elongational viscoelastic effect and a tentative explanation is offered.

AD-55-1
575

UNCLASSIFIED

SECURITY CLASSIFICATION OF THIS PAGE(When Data Entered)

TABLE OF CONTENTS

	Page
ABSTRACT.....	1
INTRODUCTION.....	2
EXPERIMENTAL PROCEDURE.....	3
TEST PROCEDURES.....	6
PRECISION AND ACCURACY OF THE DATA.....	7
RESULTS.....	11
Lift and Drag.....	11
Pressures.....	15
DISCUSSION.....	16
Separation.....	16
Boundary Layer Thinning.....	17
Viscoelastic Effects.....	18
SUMMARY AND CONCLUSIONS.....	20
REFERENCES.....	23

LIST OF FIGURES

- Figure 1 - 10-cm Chord Hydrofoil Showing Force Gauges Arrangement, Injection Slit, and Pressure Taps
- Figure 2 - Comparison Between Pressure Differences Measured by Two Different Methods During Polymer Injection Test
- Figure 3 - Comparison Between Pressure Differences Measured by Two Different Methods During a Test Without Injection
- Figure 4 - Value of the Change of the Lift Coefficient versus Incidence Angle
- Figure 5 - Change of Drag Coefficient versus Incidence Angle
- Figure 6 - Change of Drag Coefficient Components versus Incidence Angle
- Figure 7 - Pressure Coefficient With and Without Injection versus Non-Dimensional Distance. Injection at 10% Chord, Zero Incidence Angle.
- Figure 8 - Pressure Coefficient With and Without Injection versus Non-Dimensional Distance. Injection at 30% Chord, Zero Incidence Angle.
- Figure 9 - Pressure Coefficient versus Non-Dimensional Distance on Suction and Pressure Side of Hydrofoil for an Incidence Angle of $+2.5^{\circ}$. Injection at 10% Chord on the Upper Surface.
- Figure 10 - Pressure Coefficient versus Non-Dimensional Distance on Suction and Pressure Side of Hydrofoil for an Incidence Angle of -2.5° . Injection at 10% Chord on the Upper Surface.
- Figure 11 - Pressure Coefficient versus Non-Dimensional Distance on Suction and Pressure Side of the Hydrofoil for an Incidence Angle of 5° . Injection at 10% Chord on the Upper Surface.
- Figure 12 - Pressure Coefficient versus Non-Dimensional Distance on Suction and Pressure Side of the Hydrofoil for an Incidence Angle of -5° . Injection at 10% Chord on the Upper Surface.

- Figure 13 - Pressure Coefficient versus Non-Dimensional Distance on Suction and Pressure Side of the Hydrofoil for an Incidence Angle of 5° . Injection at 30% Chord on the Upper Surface.
- Figure 14 - Pressure Coefficient versus Non-Dimensional Distance on Suction and Pressure Side of the Hydrofoil for an Incidence Angle of -5° . Injection at 30% Chord on the Upper Surface.
- Figure 15 - Comparison of the Value of the Change of the Lift Coefficient Computed from Force and Pressure Measurements
- Figure 16 - Pressure Defect Measurements with a Pitot Tube Probe- Effect of Polymer Concentration
- Figure 17 - Pressure Defect Measurements with a Pitot Tube Probe- Effect of Outside Diameter of Probe
- Figure 18 - Pressure Defect Measurements with a Pitot Tube Probe- Effect of Velocity Over Outside Diameter Ratio
- Figure 19 - Absolute Change of the Lift Force versus Free Stream Velocity
- Figure 20 - Absolute Change of the Lift Force versus Local Velocity at the Injection Station
- Figure 21 - Disturbance Due to Jet Swelling

ABSTRACT

Lift and drag forces and pressure distribution were measured for a 10 cm. chord, 20 percent relative thickness, NACA 63₄-020 symmetrical, two-dimensional hydrofoil, with and without drag-reducing polymer injection. The 200 ppm solution of Polyox WSR 301 was introduced into the foil boundary layer with an injection velocity of 10 percent of the free stream velocity. The injection slits were situated at 10 and 30 percent of the chord length.

The pressure distribution data does not indicate any significant change of the separation point. It demonstrates, however, that the polymer injection always results in a significant decrease of pressure in the region aft of the injection slit.

This decrease of the local pressure gives rise to a lift increase for injections made on the suction side of the foil surface and a lift decrease for injections made on the pressure side.

The data suggest an elongational viscoelastic effect and a tentative explanation is offered.

INTRODUCTION

Significant research has been devoted to lift effects associated with drag-reducing polymers since Wu's discovery of pump effects in 1969^{(16)*}. Some of the research has involved tests on propellers^(1,2), finite span hydrofoils⁽³⁾, circular cylinders⁽⁴⁾, and two-dimensional hydrofoils⁽⁵⁾ in homogeneous polymer solutions. Other research has involved tests on hydrofoils with polymer injection on the foil surface^(6,7,8), as might actually be used in practice. In addition, tests with localized injection may facilitate separation of the different effects which can occur in homogeneous solutions, such as the leading edge and distributed surface effects.

The present tests are a continuation of earlier investigations of polymer effects on two-dimensional hydrofoils^(7,8), comprising extensive measurements of lift and drag changes over a rather wide range of injection conditions on two foils of similar shape but of different thicknesses and with a single injection position.

Past tests established that under the circumstances of these tests a lift augmentation generally occurred with injection on the upper surface of the foil. The specific purpose of the present tests was to measure the pressure changes on the foil surface

*Numbers in parentheses indicate references listed at the end of this report.

accompanying injection and lift changes. The results, described herein, are somewhat surprising as they show, in general, that maximum pressure changes occur in the region aft of, and close to, the injection slit. These data, together with a new analysis of previous lift data (which show a critical speed for onset of lift effects) seems to indicate that an elongational viscoelastic effect is involved and that the lift effects are not directly related to drag reduction.

EXPERIMENTAL PROCEDURE

The tests were performed in the HYDRONAUTICS High Speed Channel⁽⁹⁾, modified to obtain a two-dimensional flow and to eliminate the free surface effects which may otherwise have occurred at the high speeds used in these tests. This modification incorporated a roof with a specially designed transition which was attached to the original free surface sluice gate of the channel. A slightly oversized hole allows free passage of the models through the roof. The foil was supported vertically by means of a block gauge arrangement and an incidence-control system, as indicated in Figure 1. In order to eliminate air entrainment which might have been induced by low pressures on the suction side of the foil, the upper side of the roof was flooded. To create the best conditions for a two-dimensional flow and to avoid secondary flows between the lower and upper section of the roof, an end plate was fitted to the cross section of the foil, being free to move with it (Figure 1). This arrangement did not completely eliminate the secondary flow and did not restore a completely parallel flow. The testing set-up has previously been used in extensive strut testing at HYDRONAUTICS and is thoroughly discussed elsewhere⁽¹⁰⁾. It is believed to be suitable for these comparative measurements of the hydrodynamic characteristics of foils with and without injection.

The foil used in this investigation was a NACA 63 symmetrical profile, 10.16 cm. in chord with 20 percent maximum relative thickness at 30 percent of the chord. Spanwise injection slits were situated at 10 and 30 percent chord distance from the leading edge. Ten pressure taps were arranged diagonally on each side of the foil at an angle of 52 degrees to the stream so that the downstream influence of each on the others was minimized. The pressure taps extended approximately from 20 percent to 90 percent chord and were 1.01 mm. in diameter.

The injection slits were designed so as to minimize possible local perturbations produced by the ejected fluid. The inclination of the slits, relative to the foil tangent at the injection station, was 7 degrees for both foils. Based on an empirical relationship describing the diffusion of a dilute polymer solution over a flat plate obtained by Fruman and Tulin⁽¹¹⁾ the gap of the injector was selected to be 0.0127 cm. For reference, the estimated sub-layer thickness at a speed of 11m/sec in water without additives is 0.003 cm.

The foil was fabricated from aluminum and then chrome plated. A silicone spray was applied to the surface of the foil in order to preserve the quality of the finish.

The free stream velocity in the test section was measured with a 3 mm. diameter Prandtl tube placed ahead of the hydrofoils. Though it is known, in general, that the stagnation pressure readings of such tubes are affected by polymer solutions, it is certain that in the present case the relatively small buildup of polymer concentrations (less than 1 ppm) in the recirculating water make any significant errors highly improbable.

The lift and drag forces were measured by means of four reluctance-type block gauges, HYDRONAUTICS Modular Force Gauge

Model H1-M-2, attached to the foils as shown in Figure 1. The total lift and drag load capacities of these gauges were 100 and 25 kg, respectively. The gauges were individually calibrated prior to the tests. After mounting the gauges, a new recalibration was performed to account for any possible interaction. During the tests, the electrical output signal from the gauges was integrated over a ten-second period and the average values were recorded.

The pressures were measured by means of three diaphragm pressure transducers, Pace Engineering Co., coupled to a scanner, Scanivalve Model WSG-12. Two of the transducers, with a capacity of 10 psi, measured the pressures on both sides of the foil surfaces, while the third transducer, with a capacity of 5 psi measured the pressure differential between either side of the foil surface. A static pressure tap in the bottom of the channel was used as reference for the first two transducers. The pressure transducers were also calibrated prior to the tests. An arrangement similar to the one used for the force gauges provided for average pressure reading over a ten-second period.

The injected fluids were contained in a nine-gallon reservoir, which was pressurized so as to drive the fluids into the injection slit through a pipe system. The pipe system contains a regulating valve and a rotameter for the determination of the flow rate. The rotameter was calibrated with water only, but was also used for the polymer solutions. Independent checks showed that the rheological characteristics of the dilute polymer solution do not affect the calibration of the rotameter. Degradation of the polymer solution can occur due to the shear stresses applied to it when flowing from the reservoir into the injection slit. The level of degradation was checked by flowing through the injection system a virgin solution of polymer at two different

flow rates. The solutions so circulated were collected and tested for their drag reduction properties in a 3 mm. diameter stainless steel pipe. The results of these tests demonstrated no noticeable decrease of the drag reduction properties of the circulated solutions when compared to the virgin solution. It was therefore considered that the injection system does not introduce a degradation of the polymer solutions capable of significantly affecting the experimental results. The ratio between the injection velocity and the free stream velocity, the "rate of injection," was kept constant at 0.1 throughout the test.

The polymer used in these tests was poly (ethylene oxide), POLYOX WSR 301*, which has been demonstrated to be a highly efficient drag-reducing agent in internal and external flows⁽¹¹⁾. The solutions were always prepared in a concentrated form (1000 ppm), the day before utilization, by gently mixing the dry powder with the necessary amount of tap water. No specific precautions were taken to limit biological degradation of the solutions.

TEST PROCEDURES

For all tests a specific procedure was followed in order to eliminate possible errors and increase the degree of confidence in the results. Before any injection test, the specified hydrofoil incidence angle was set and the free stream velocity was established in the recirculating water channel. This velocity was continuously monitored throughout the test. The standard deviation in the mean value of the velocity for a series of ten measurements was about 0.25 percent. After setting

* Manufactured by Union Carbide Corporation.

the velocity, a first series of measurements of the velocity and the lift and the drag forces was performed. The fluid was then injected and upon stabilization of the lift and drag voltmeters a record of the displayed values was taken. A new measurement was made about ten seconds later. The injection was then discontinued and upon stabilization of the digital voltmeter a reading of the parameter values without injection was taken again.

During the experiments conducted to measure the pressure distribution the above procedure was repeated for each pair of pressure taps. The pressures were recorded once without any injection, twice during injection and once again without injection. This test procedure is believed to insure the reliability of the data.

The question of precision and accuracy of the data is discussed below.

PRECISION AND ACCURACY OF THE DATA

The objective of the test program was to investigate the relative changes caused in the hydrodynamic forces and the pressure distribution between an injection of water and dilute polymer solution; for a proper assessment of these small changes, it is essential to ascertain the basic accuracy and degree of repeatability of the measurements under conditions of zero injection.

Sources of experimental error are inadequacies in the measuring equipment (such as the force gauges and the pressure transducers), unsteadiness of flow conditions ahead of the hydrofoils (turbulence as well as low-frequency fluctuations) and model deflection under loads.

The force gauges are sufficiently linear in the operating range of the tests for any errors due to nonlinearities to be negligibly small. Moreover, since the force measurements are obtained from a ten-second integration of the instantaneous gauge output, errors due to high-frequency velocity fluctuations are unlikely. The above applies also to the velocity fluctuations which are integrated during a ten-second period. In a previous paper⁽⁷⁾, the question of repeatability of the tests was analyzed. It was concluded then that the lift and drag coefficients can be expected to be reproducible within a variation range of ± 2 percent. This question has been further investigated during the present research phase. Table 1 shows the values of the mean velocity, and the mean lift and drag coefficients without injection resulting from the twenty individual measurements performed during each test. Also the associated standard deviation in percent is shown in the same table. In considering this table it can be seen that the standard deviation associated with the velocity fluctuation was always well below 1 percent and generally below 0.25 percent. The force coefficients did not show much larger standard deviations.

If the values of the force coefficients for the same incidence angle are considered all together, they show for 5 degrees incidence a standard deviation of 3.2 percent; while for an incidence of 2.5 degrees, the standard deviation is 2.6 percent. The drag coefficients show standard deviations of 3.8 percent and 1.0 percent for 5 degrees and 2.5 degrees, respectively.

The mean drag coefficient for zero incidence angle for six tests comprising twenty individual measurements each is 0.01415 with a standard deviation of 1.4 percent. For standard roughness and Reynolds numbers of 6.0×10^6 , the drag coefficient of a

TABLE 1
Mean Values and Standard Deviation for the
Velocity and the Lift and Drag Coefficients

Test No.	Date	Incidence Angle, °	Velocity		Lift Coefficient		Drag Coefficient	
			Mean, m/sec	Standard Deviation, %	Mean	Standard Deviation, %	Mean	Standard Deviation, %
3	10/28/74	5.00	10.978	0.07	0.3203	0.47	0.0293	0.37
4	10/28/74	5.00	10.981	0.14	0.3206	0.59	0.0293	0.51
5	10/28/74	-5.00	10.964	0.11	-0.3138	0.70	0.0316	0.35
6	10/28/74	-5.00	10.981	0.14	-0.3141	0.61	0.0317	0.28
10	10/28/74	5.00	10.963	0.14	0.3169	0.40	0.0294	0.37
11	10/28/74	5.00	10.971	0.34	0.3179	0.31	0.0295	0.33
13	10/29/74	-5.00	10.983	0.20	-0.2928	0.55	0.0295	0.50
14	10/29/74	-5.00	10.935	0.18	-0.2943	0.72	0.0291	1.37
18	10/29/74	5.00	10.979	0.19	0.3073	0.74	0.0283	0.84
19	10/29/74	5.00	10.976	0.24	0.3057	0.50	0.0286	0.59
20	10/31/74	2.50	10.958	0.13	0.1241	0.95	0.0179	0.55
22	10/31/74	2.50	10.939	0.15	0.1242	0.65	0.0182	0.55
23	10/31/74	-2.50	10.981	0.21	-0.1218	1.06	0.0176	0.40
25	10/31/74	-2.50	10.978	0.83	-0.1236	1.23	0.0180	0.28
26	10/31/74	-2.50	10.966	0.22	-0.1256	1.63	0.0178	0.34
27	11/1/74	-2.50	10.950	0.17	-0.1246	1.63	0.0180	0.27
28	11/1/74	2.50	10.970	0.18	0.1310	0.97	0.0182	0.50
29	11/1/74	2.50	10.982	0.12	0.1303	0.58	0.0181	0.33

very similar foil (634-021) given in Reference 12 is 0.011. The 30 percent larger values measured during the present tests can be ascribed to some of the experimental problems discussed earlier.

In conclusion, during a given test, the velocity and forces on the hydrofoil are very stable with standard deviations below 1 percent. Between tests, the force coefficients show more significant differences which may be as high as 3.8 percent. These differences are mainly due to the difficulty of precisely reproducing the incidence angle of the foil. This latter aspect of the problem does not have any direct bearing on the analysis of the results, since the tests with and without injection are made without changing the hydrofoil angle setting.

The pressure gauges were checked for proper operation by comparing the difference between the pressures measured with two of the gauges against the pressure differential of the third gauge. Figures 2 and 3 show the agreement between both measurements for a foil incidence of 5 degrees and a velocity of 11 m/sec with and without injection.

Another way to check for the precision of the pressure measurements is to consider the lift coefficients computed from the force measurements with the lift coefficients obtained from the integration of the pressure coefficients. The pressure distribution on both sides of the foil surface for a given lift coefficient can be computed, for an inviscid and unbound flow, using the procedure given in Reference 12. Figure 3 shows the agreement between the computed pressure difference between both surfaces of the foil and the experimental results. The percent of total lift contributed by the differential pressure distribution between the first and the last pressure taps is 51.47

in the case of the theoretical computation and 47.32 in the case of the experimental results. The difference between both values is small and may result from several factors such as boundary layer and separation effects on the pressure distribution, especially over the last 30 percent of the chord and the wall effect due to the limited width of the channel. It would seem from the above that the pressure measurements are well within the range of unavoidable experimental errors.

RESULTS

Lift and Drag

The effect of injection on both lift and drag coefficients of the hydrofoil is summarized in Table 2, where injection is always made on the upper surface and the lift is always measured positive upwards. In eight out of ten measurements the injection of water created a down force, as might normally be expected from a jet flap effect.

In every case, the injection of polymer caused an upward force relative to the water injection case, the magnitude generally increasing with incidence and being greater in the case of the 10 percent injection position than for 30 percent. The difference between lift coefficients measured with polymer injection and no injection at all, ΔC_L , is plotted in Figure 4. Over the range of incidence used, the pressure coefficients are always negative in the region of injection, their magnitude increasing with incidence. The lift results therefore suggest a dependency of the polymer effect on the local velocity in the region of injection, and/or a possible dependency on the velocity gradients over the upper foil surface; this dependency will be discussed later.

TABLE 2
Change of the Lift and Drag Coefficients
for Water and Polymer Injection

Angle (Deg)	Inject. Station	Inject. Rate	Lift Coefficient			Drag Coefficient				
			Water		Polyox	Water		Polyox		
			Change	%	Change	%	Change	%		
5	0.1	0.1	-0.00238	-0.74	+0.0276	+ 8.73	-0.00016	-0.55	+0.00141	+4.7
2.5	0.1	0.1	-0.00284	-2.16	+0.0146	+11.74	-0.00023	-1.27	-0.000331	-1.84
0	0.1	0.1	-0.00380	-	+0.00858	-	-0.00006	-0.45	-0.00111	-7.62
-2.5	0.1	0.1	-0.00252	-2.01	+0.00945	+ 7.75	+0.000055	+0.31	-0.00123	-6.97
-5.0	0.1	0.1	-0.0022	-0.70	+0.00592	+ 2.02	+0.00010	+0.31	-0.00148	-5.0
5	0.3	0.1	-0.00139	-0.44	+0.01268	+ 4.31	-0.00010	-0.31	+0.00013	+0.44
2.5	0.3	0.1	+0.00172	+1.32	+0.00867	+ 7.01	-0.000152	-0.84	-0.00032	-1.76
0.0	0.3	0.1	-0.00204	-	+0.00494	-	-0.000077	-0.53	-0.00078	-5.30
-2.5	0.3	0.1	+0.00111	+0.89	+0.0058	+ 4.67	-0.000157	-0.87	-0.00104	-5.70
-5.0	0.3	0.1	-0.00197	-0.61	-0.00043	- 0.13	+0.00015	+0.51	-0.00021	-0.71

The change in the drag coefficient, ΔC_D , shown in Figure 5 is, in the case of a two-dimensional foil, composed of two terms, ΔC_{D_f} the friction drag, and ΔC_{D_p} the pressure drag, where:

$$\begin{aligned}\Delta C_D &= C_D (\text{polymer}) - C_D (\text{water}) \\ &= \Delta C_{D_f} + \Delta C_{D_p}\end{aligned}$$

The rapid rise in ΔC_D , to positive values as incidence increases, suggests a pressure drag effect due to the reduced surface pressures acting over the rearward sloping portion of the foil. These can be estimated by integration of the product of measured pressures and slopes, assuming that no pressure changes occur outside of the region of the pressure taps (20-90 percent chord). The results are shown in Table 3 together with the friction drag changes deduced by subtracting the calculated estimates of ΔC_{D_p} from the measured values of ΔC_D , and they are plotted in Figure 6.

The roughly parabolic shapes of the pressure drag curves reflects the roughly linear increase of the lift changes with incidence shown in Figure 4. The generally smaller pressure drag for the .1 chord injection position reflects the fact that the slope of the foil is forward facing for positions upstream of the .3 chord at zero and negative incidence. For the higher positive angles of attack the forward thrust effect disappears, as the data indicate. The deduced values of friction drag are shown always to be reduced by the additive, and by a greater amount in the case of the .3 chord injection than for the .1 position, an effect which is contrary to expectation and which remains unexplained. It must be remembered though, that the decomposition of ΔC_D is very sensitive to pressure changes over the nose of the hydrofoil, should they occur.

TABLE 3
Friction and Pressure Components
of the Drag Coefficient

Angle	Inject. Station	ΔC_D	ΔC_{D_P}	ΔC_{D_f}
5	0.1	+0.00141	+0.002054	-0.000664
2.5	0.1	-0.000331	+0.000405	-0.000736
0	0.1	-0.00111	+0.000015	-0.00112
-2.5	0.1	-0.00123	-0.000815	-0.000415
-5.0	0.1	-0.00148	-0.00089	-0.000591
5	0.3	+0.00013	+0.001721	-0.001851
2.5	0.3	-0.00032	+0.001357	-0.001677
0	0.3	-0.00078	+0.000538	-0.001318
-2.5	0.3	-0.00104	+0.000348	-0.001388
-5.0	0.3	-0.00021	+0.000025	-0.000235

The friction drag coefficient for the foil, estimated from a turbulent friction curve, is approximately 0.009, so that the estimated changes in friction drag coefficient in the range .0005 to .002 correspond approximately to a 10-40 percent friction reduction, when account is taken that injection occurs on one side only. The larger value corresponds to the .3 injection position and is in accord with drag reduction estimates which can be made using the result of (11), but the lower value, for the .1 position, is only about 25 percent of the estimate.

Pressures

The pressures measured on the injection side of the foil at zero incidence are shown in Figures 7 and 8, for the cases with and without polymer injection and for the two injection positions. In both cases, the pressures aft of the injection slit are significantly reduced when injection occurs, the reduction falling toward the rear of the foil. The pressure changes upstream of the .3 chord slit are generally small. During these tests the pressures on the foil surface opposite to injection were also measured. In the case of the .3 slit, the effect of polymer injection on these latter pressures was negligible, i.e., generally within the repeatability of the measurements (about .002 in C_p). In the case of the .1 slit, however, there seems to be a perceptible reduction in the magnitude of C_p (an increase in pressure) on the lower surface in the region between 0.1 and 0.5 chord, during injection on the upper surface; the average value of this change in C_p is about -0.008. Similarly, the data for other angles of attack, Figures 9-14, show a negligible effect of injection on bottom surface pressures for injection at .3c, but a noticeable effect for injection at .1c, except for $\alpha = -5^\circ$, the effect seeming to increase with increasing incidence.

A comparison of the absolute values of the lift coefficients computed from the force gauge measurements with those computed from the pressure measurements indicates, Figure 15, that the latter values somewhat overestimate, in general, the effect of polymer injection. This overestimation may be due again to neglect of pressures on that portion of the foil surface forward of .187 chord, implying increased values there as a consequence of injection.

One additional feature of the measured pressure changes deserves mention, the rather large variation from point to point. Whether these are an artifact of the measurement technique or have a cause in the phenomena involved is not, at present, clear. The apparent scatter does, however, seem to be greater than the estimated resolution in C_p (.002) would suggest.

DISCUSSION

Different hypotheses can be advanced to explain how polymers alter pressure distributions and lift forces on two-dimensional hydrofoils. Hypotheses relating such effect to a change in the separation point, to asymmetric boundary layer thinning and to some kind of viscoelastic effect have been suggested. These possibilities are briefly discussed below, with an emphasis on viscoelastic phenomena.

Separation

The pressure distributions shown previously here do not seem to show any changes which can clearly be identified as affecting separation favorably. The fact that the pressure changes tend to occur most generally and in greatest magnitude just aft of the injection slits, make it difficult to ascribe the changes to separation effects.

Boundary Layer Thinning

The pressure distribution on a hydrofoil is effected by the boundary layer. This effect may be taken into account by considering the hydrofoil shape to be altered by the displacement thickness of the boundary layer. Drag reduction and subsequent boundary layer thinning on the upper surface, only, of a symmetrical foil will therefore produce a lift force. The magnitude of this force can be estimated by imagining a change in incidence, $\Delta\alpha$, related to the change in δ^* , the displacement thickness at the trailing edge of the foil, and multiplying $\Delta\alpha$ by an appropriate lift curve slope, $\Delta C_L/\Delta\alpha$.

$$\Delta\alpha = \frac{\Delta\delta^*}{C} 57.3 \text{ (degrees)}$$

$$\frac{\Delta\delta^*}{C} \approx (1.2) \cdot \frac{\Delta C_f}{\theta}, \text{ according to simple momentum theory}$$

and where we assume $\delta^* = 1.2\theta$, and θ is the momentum thickness.

$$\text{Using } \Delta C_L/\Delta\alpha = .08/\text{degree},$$

$$\Delta C_L \approx 3 \Delta C_f$$

These values are tabulated below, using ΔC_f values from Table 3.

α	Inj. Sta.	ΔC_{L_f} (friction)	ΔC_{L_m} (measured)	$\Delta C_{L_m} - \Delta C_{L_f}$
+5	0.1	+0.0020	+0.0276	+0.0256
+2.5		+0.0022	+0.0146	+0.0124
0		+0.0034	+0.0086	+0.0052
-2.5		+0.0012	+0.0095	+0.0083
-5		+0.0018	+0.0059	+0.0041
+5	0.3	+0.0055	+0.0127	+0.0072
+2.5		+0.0050	+0.0087	+0.0037
0		+0.0039	+0.0049	+0.0010
-2.5		+0.0041	+0.0058	+0.0017
-5		+0.0007	-.00043	-.0011

The Table shows that the lift induced by boundary layer thinning could be most important in the case of .3 chord injection and least in the case of .1 chord injection and $\alpha = 5^\circ$. This conclusion is in contrast with the changes in bottom pressures due to injection, which were negligible for .3 chord injection and greatest for .1 chord injection and $\alpha = 5^\circ$. Neither would the changes in pressure due to boundary layer thinning be greatest just aft of the injection slit and very small before. It is therefore difficult to ascribe the major effects observed to this cause.

Viscoelastic Effects

It is well known that dilute polymer solutions can display viscoelastic behavior when subjected to elongational flows such as those produced in the stagnation region of a Pitot tube probe or when exiting from a tube⁽¹³⁾. In the former case the viscoelastic effect can cause loss of head as measured by the Pitot tube^(14,15). This loss has been extensively studied in experiments at HYDRONAUTICS by Wu and at the University of Orsay (France) by Fruman and colleagues, and theoretically by Tulin at HYDRONAUTICS. The latter predicted that the anomalous pressure head would occur only for super-critical values of a non-dimensional parameter $\frac{U}{d} \tau_R$ where U is a characteristic flow velocity, d a characteristic length, and τ_R the polymer relaxation time. He further predicted that the anomalous pressure would increase linearly with the logarithm of values of this parameter greater than critical. Both the data of Wu and Fruman, et al., vary in this way for parameter values that are not too large. In Figures 16-18, the measured pressure defects are shown plotted versus the logarithm of the free stream velocity. As demonstrated through a comparison of Figures 17 and 18, the data for different probe sizes is very nearly collapsed through use of the parameter U/d .

The above observations suggested to us to plot the data for added lift due to polymer injection in the same way (i.e., lift force vs. logarithm of the free stream velocity, V). The data from a previous paper ⁽⁷⁾ are shown plotted in this way in Figure 19. The law of logarithm linearity with velocity is demonstrated but the critical velocities are dependent on foil angle. This dependency is completely eliminated by replacing the free stream velocity with the local velocity V_i , at the injection station, deduced from the measured pressure coefficients, as shown in Figure 20. The critical velocity is seen to be 9 m/sec; a value larger by an order of magnitude than the critical velocity for drag reduction as can be calculated from

$$\frac{u^{*2} \tau_R}{\nu} \approx 1$$

$$\rho u^{*2} = \tau_w = \rho V^2 \cdot C_f$$

where u^* and τ_w are the shear velocity and stress, respectively and ρ the specific mass of the fluid. For $C_f = .0045$, $\mu = 10^{-2}$ (cgs), and $\tau_R = 2 \times 10^{-3} \text{ sec}^{-1}$,

$$U_{\text{crit}} = \left(\frac{\mu}{C_f \cdot \tau_R} \right)^{\frac{1}{2}} = \left(\frac{10^{-2}}{4.5 \times 10^{-3} \times 2 \times 10^{-3}} \right)^{\frac{1}{2}} \\ = 33 \text{ cm/sec.}$$

This result further suggests that the drag reduction phenomena itself is not directly related to the lift effect, but is fundamentally different.

The characteristic length for an elongational viscoelastic phenomena with a critical speed (equal to the injection velocity) of 0.7 m/sec and for a polymer relaxation time of 2×10^{-3} is

$$l = U_{\text{crit}} \times \tau_R = 0.7 \times 10^2 \times 2 \times 10^{-3} \approx 1.4 \text{ mm}$$

This is much smaller than the distance downstream of the slit exit over which the turbulent diffusion of polymer is very small (i.e., over which the polymer jet remains coherent), according to (14). This latter distance is given there, according to Figure 12 of that reference, as

$$l \approx 10 \times C_1 \times S \times \left(\frac{v_1}{V_1} \right)^{1.5} = 10 \times 200 \times 1.2 \times 10^{-2} \times (.03) = 7 \text{ mm}$$

where v_1 is the injection velocity, S the slot width, and C_1 the concentration.

This fact suggests the speculation that the injected polymer swells over a distance of about 2mm. from the injection slit, creating a local disturbance, as shown in Figure 21. This disturbance would tend to effect bottom pressures much more in the case of .1 injection than for the .3 case, as observed.

This hypothesis needs much more scrutiny. Leaving it aside, however, the form of the lift vs. velocity curves, Figure 20, strongly suggests that the origin of the lift and pressure changes due to polymer injection lies in some kind of elongational visco-elastic effect.

SUMMARY AND CONCLUSIONS

1. Measurements of lift, drag and local pressures have been made on a symmetrical hydrofoil of 10 cm chord and 20 cm span with a 63₂-020 section at a water channel speed of 11 m/sec, with and without injection of both water and drag reducing polymer.

2. The hydrofoil was equipped with an end plate and the flow at the center of the hydrofoil was essentially two-dimensional.

3. The spanwise injection slit, inclined at 7 degrees to the local surface, had a .012 cm gap and was located at 10 and 30 percent aft of the foil leading edge.

4. The polymer was WSR 301, injected at a concentration of 200 ppm and with a velocity of 1.1 m/sec.

5. The injection of water on the upper surface generally resulted in a downward force component; the largest measured change in C_L was .0038.

6. The injection of polymer on the upper surface generally resulted in an upward force component, increasing in magnitude with increasing incidence to a maximum value for ΔC_L of .028 for $\alpha = 5^\circ$ and the .1 chord injection position; the lift augmentation is significantly greater in the case of the forward injection position.

7. The pressure changes in the case of polymer injection are generally most pronounced just aft of the injection slit and decay with distance downstream.

8. In the case of the aft injection position, changes in pressure forward of the slit on the foil bottom are small or negligible.

9. In the case of the forward injection position, changes in pressures on the foil bottom are not negligible and increase with incidence.

10. The maximum measured change in pressure coefficient was about .04 or about 40 psf.

11. The major effects of polymer injection on surface pressures and lift are not due to alteration of boundary layer separation position or to boundary layer thinning accompanying drag reduction.

12. The lift augmentation exhibits a critical speed based on local velocities on the foil surface, below which lift augmentation does not occur; the critical speed was 9 m/sec under the conditions of the present tests.

13. The lift augmentation varies with the logarithm of the local velocity for speeds in excess of critical.

14. The data suggest that lift and pressure changes due to polymer injection are due to an elongational viscoelastic effect.

15. The suggestion is made that the effects are related to swelling of the polymer jet within a few millimeters of the injection slit.

16. Much more experimental research needs to be done in order to further elucidate these effects and determine their practical application.

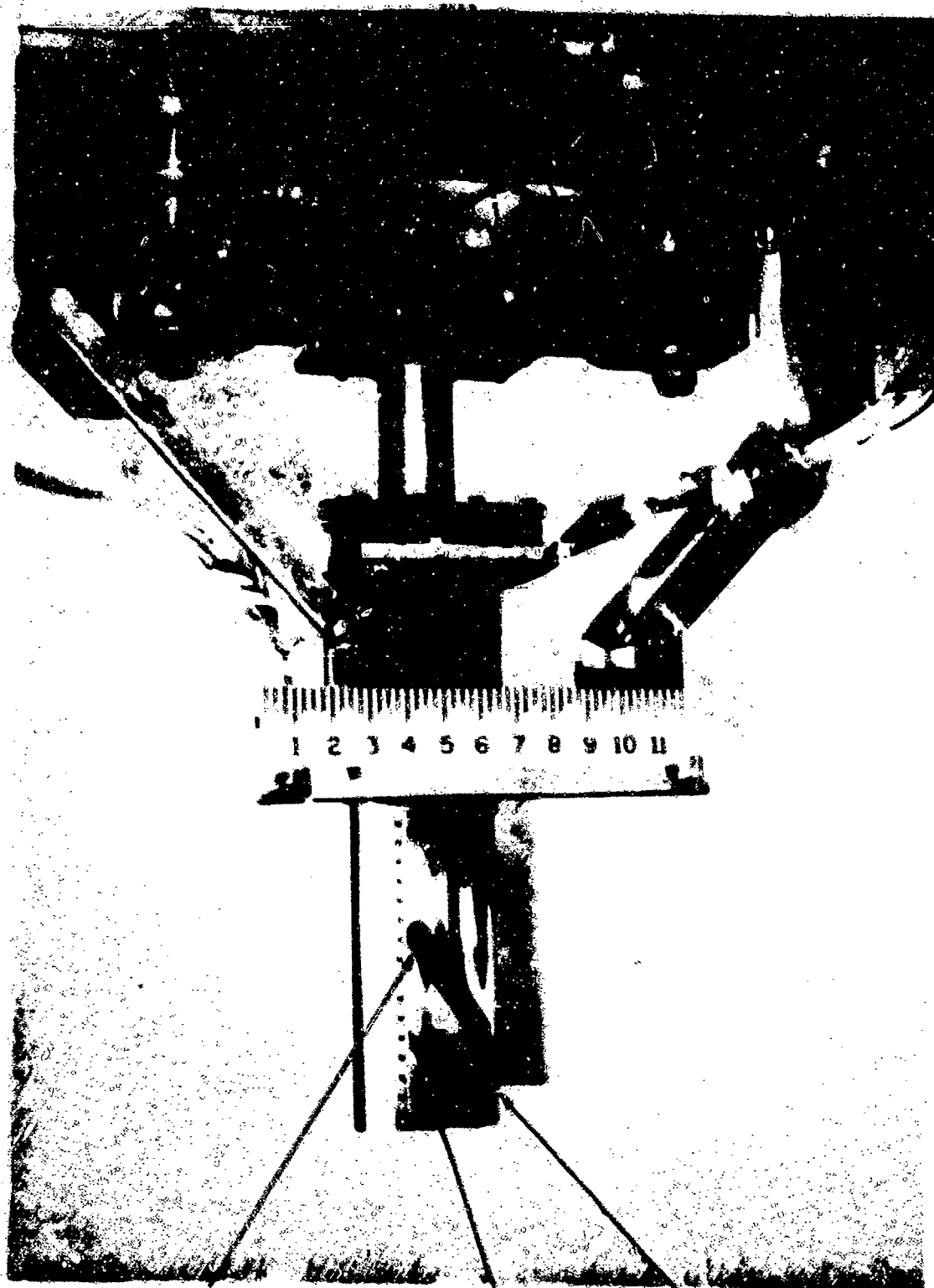
REFERENCES

1. Kowalsky, T., "Effect of Polymer Additives on Propeller Performance," J. Hydronautics, Vol. 5, No. 1, January 1971.
2. Henderson, L. H., "Effects of Polyethylene-Oxide Solutions on the Performance of a Small Propeller," Thesis, U. S. Naval Postgraduate School, September 1971.
3. Wolf, J. H. and Cahn, R. D., "Lifting Surfaces in Polymer Solutions," NSRDC Report 3653, May 1971.
4. Sarpkaya, T. and Rainey, P. E., "Flow of Dilute Polymer Solutions about Circular Cylinders," U. S. Naval Postgraduate School, NPS-59SL1021A, February 1971.
5. Sarpkaya, T., "On the Performance of Hydrofoils in Dilute Polyox Solutions," International Conference on Drag Reduction, Cambridge, England, September 1974.
6. Lehman, A. F. and Suessmann, R. T., "An Experimental Study of the Lift and Drag of a Hydrofoil with Polymer Ejection," Oceanics, Incorporated, Report Number 72-94, November 1972.
7. Fruman, D. H., Sundaram, T. R. and Daugard, S. J., "Effect of Drag Reducing Polymer Injection on the Lift and Drag of a Two-Dimensional Hydrofoil," International Conference on Drag Reduction, Cambridge, England, September 1974.
8. Fruman, D. H., "Lift Effects Associated with Drag Reducing Polymer Injection on Two-Dimensional Hydrofoils," 1974 Annual Meeting of the Ordnance Hydroballistics Advisory Committee, Newport, Rhode Island, October 1974. Submitted for Publication to the Journal of Ship Research.
9. Johnson, V. E., Jr. and Goodman A., "The HYDRONAUTICS, Incorporated Variable-Pressure, Free-Surface, High-Speed Channel," Cavitation Research Facilities and Techniques, ASME, New York, p. 49, 1964.
10. Etter, R. J. and Huang, T. T., "An Experimental Investigation of the Static Hydrodynamic Characteristics of Several Faired Cables Having Symmetrical NACA Airfoil Sections," HYDRONAUTICS, Incorporated Technical Report 530-1, July 1967.

11. Fruman, D. H. and Tulin, M. P., "Diffusion of a Tangential Drag-Reducing Polymer Injection on a Flat Plate at High Reynolds Numbers," 1974 Annual Meeting of the Ordnance Hydroballistics Advisory Committee, Newport Rhode Island, October 1974. Submitted for Publication to the Journal of Ship Research.
12. Abbott, I. H., von Doenhoff, A. E. and Stivers, L. S., "NACA Wartime Report," ACR Number L5C05, March 1945.
13. Tulin, M. P., "Hydrodynamic Aspects of Macromolecular Solutions," Sixth Symposium on Naval Hydrodynamics, ACR-136, Office of Naval Research, Department of the Navy, Washington, D. C., pp. 3-19, 1966.
14. Smith, K. A., Merrill, E. W., Mickley, H. S., and Virk, P. S., "Anomalous Pitot Tube and Hot Film Measurements in Dilute Polymer Solutions," Chemical Engineering Science, Volume 22, pp. 619-626, 1967.
15. Fruman, D. H., Loiseau, G., and Sulmont, P., "Effects Visco-elasticity dans les Mesures des Pressions Statiques et d'Arret," La Houille Blanche, Number 5, pp. 445-452, 1970.
16. Wu, Jin, "Lift Reduction in Additive Solutions," Journal of HYDRONAUTICS, Volume 3, Number 4, pp. 193-200, October 1969.

HYDRONAUTICS, INCORPORATED

FORCE
GAUGES



PRESSURE TAPS

30% CHORD
INJECTION SLIT

FOIL

FIGURE 1 - 10-cm CHORD HYDROFOIL SHOWING FORCE GAUGES
ARRANGEMENT, INJECTION SLIT, AND PRESSURE TAPS

HYDRONAUTICS, INCORPORATED

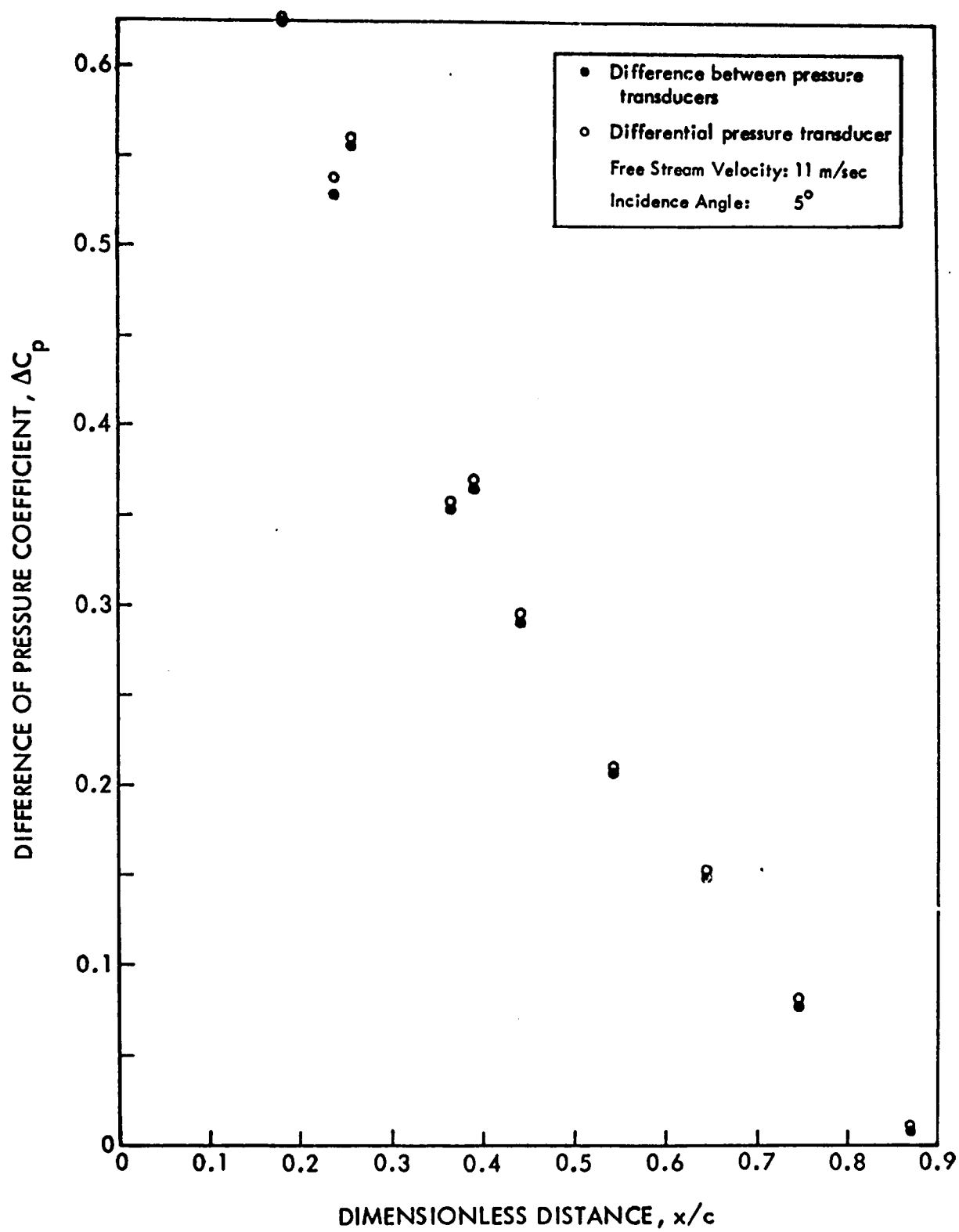


FIGURE 2 - COMPARISON BETWEEN PRESSURE DIFFERENCES MEASURED BY TWO DIFFERENT METHODS DURING POLYMER INJECTION TEST

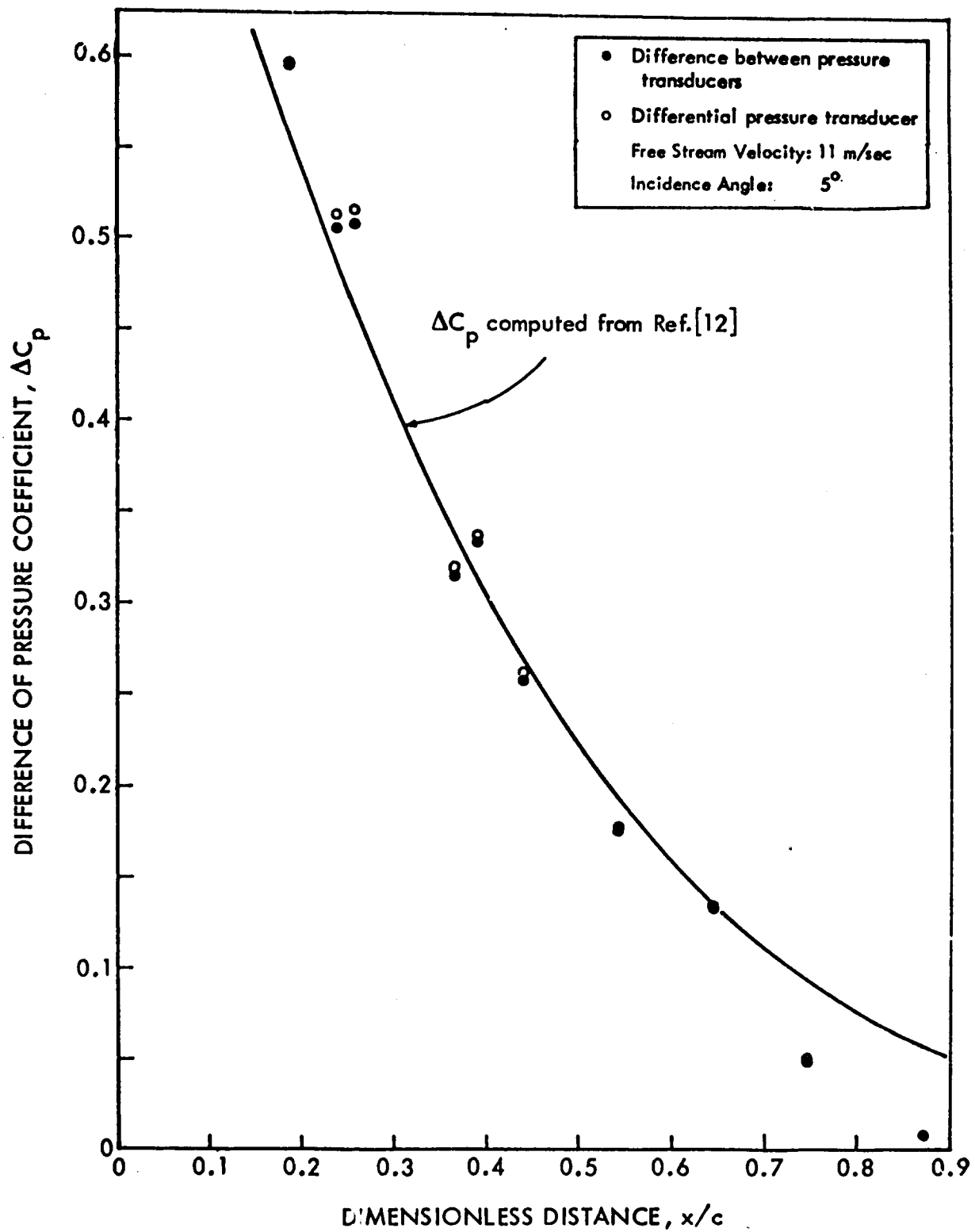


FIGURE 3 - COMPARISON BETWEEN PRESSURE DIFFERENCES MEASURED BY TWO DIFFERENT METHODS DURING A TEST WITHOUT INJECTION

HYDRONAUTICS, INCORPORATED

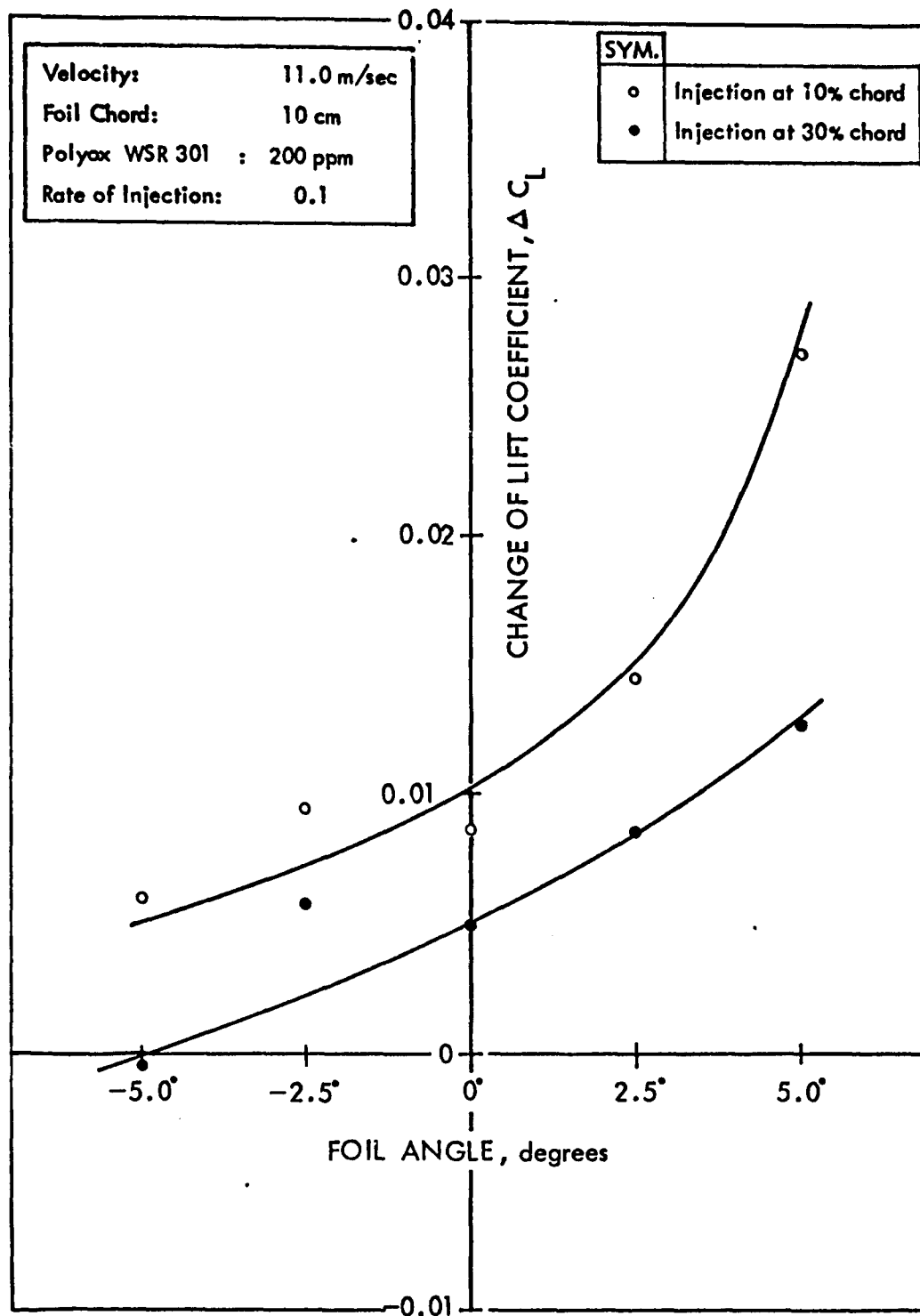


FIGURE 4 - VALUE OF THE CHANGE OF THE LIFT COEFFICIENT
VERSUS INCIDENCE ANGLE

HYDRONAUTICS, INCORPORATED

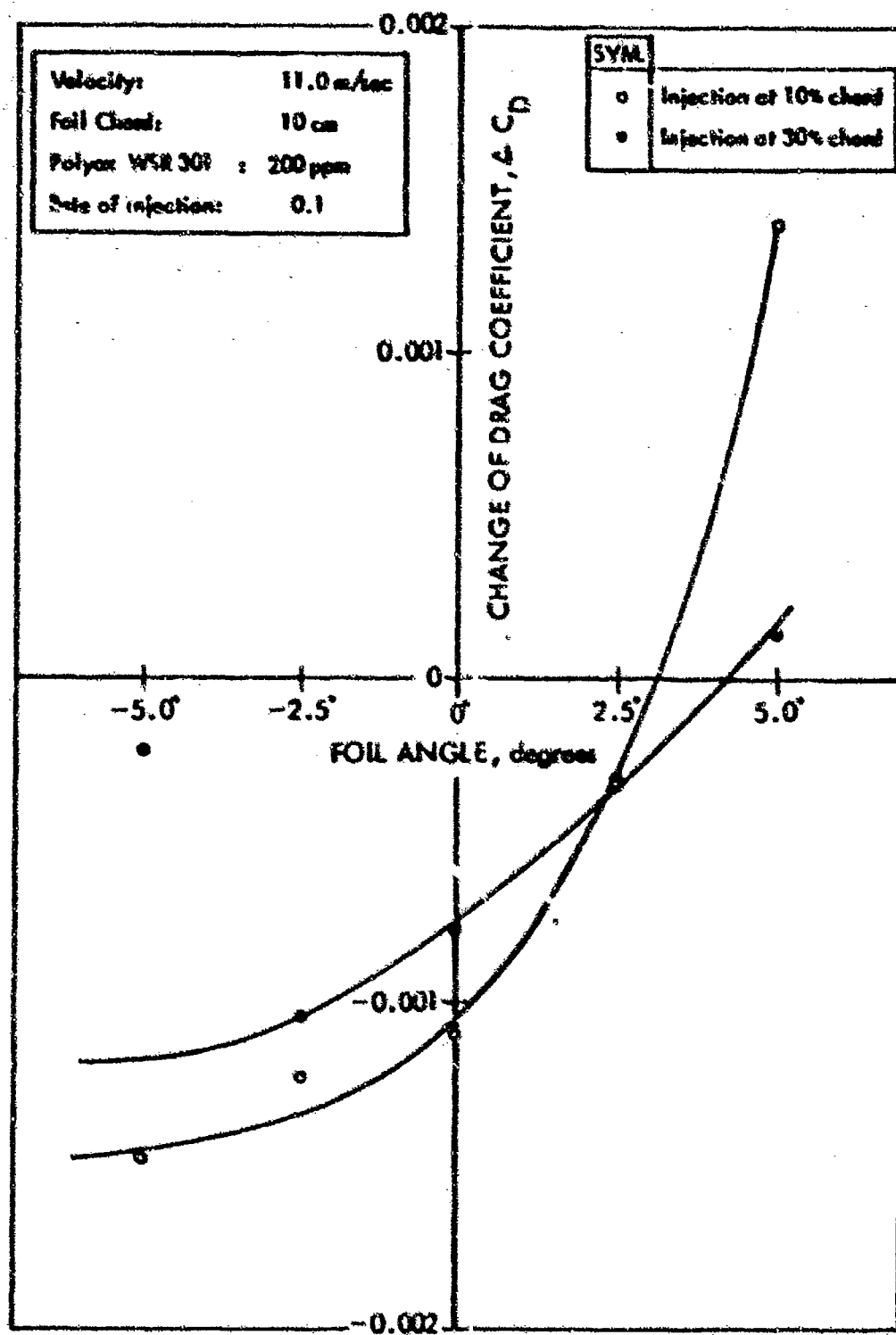


FIGURE 5 - CHANGE OF DRAG COEFFICIENT VERSUS INCIDENCE ANGLE

HYDRONAUTICS, INCORPORATED

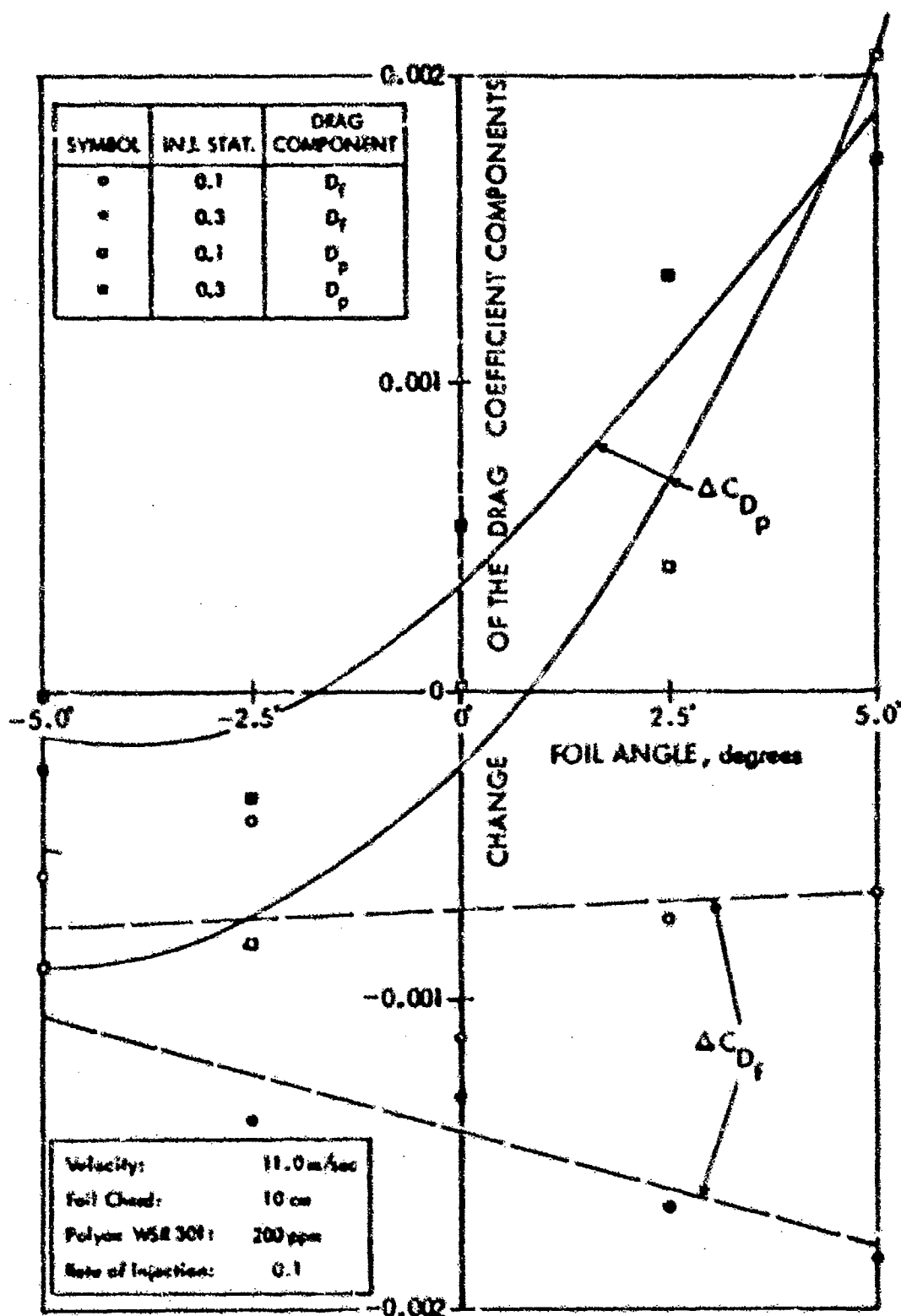


FIGURE 6 - CHANGE OF DRAG COEFFICIENT COMPONENTS VERSUS INCIDENCE ANGLE

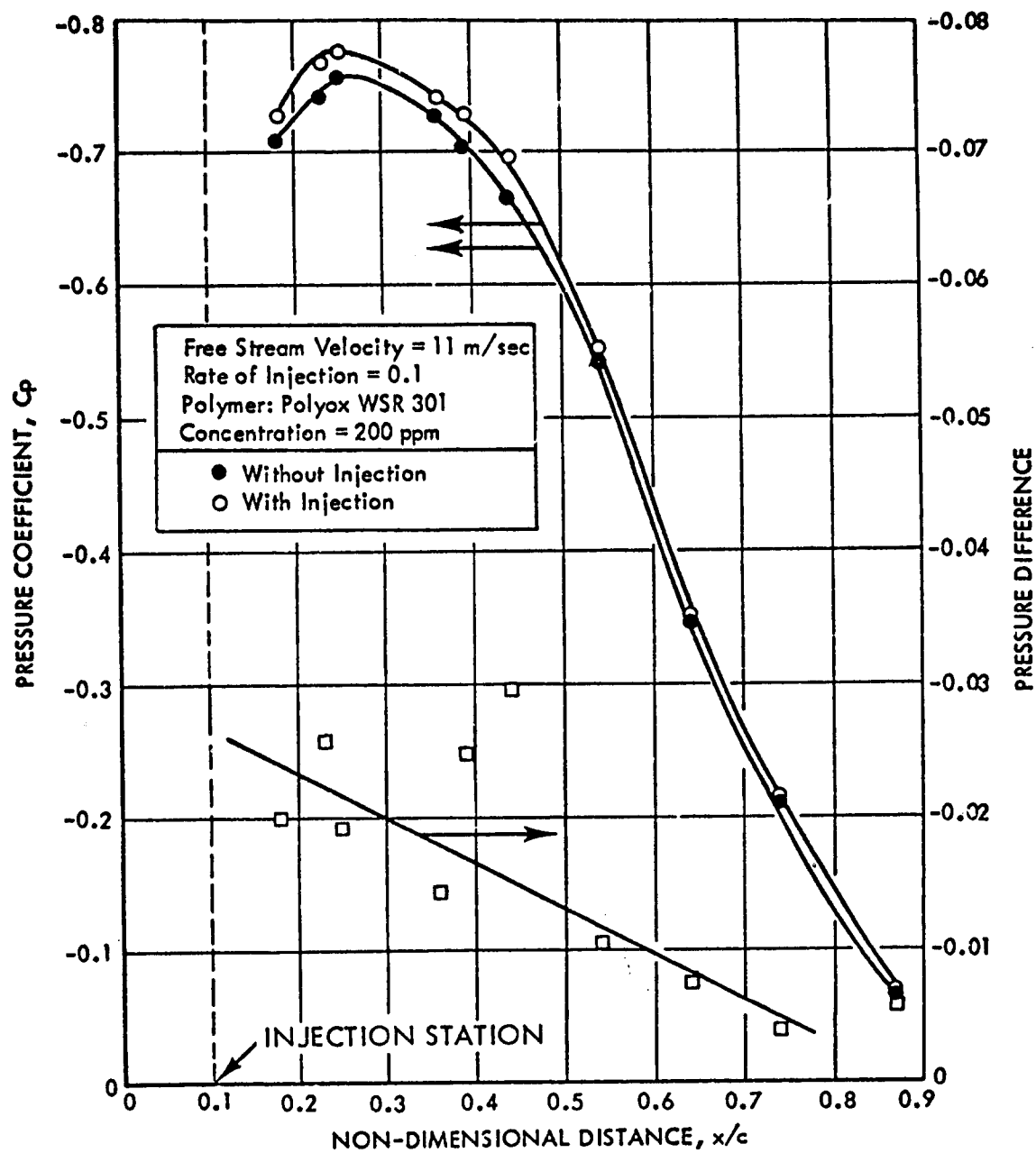


FIGURE 7 - PRESSURE COEFFICIENT WITH AND WITHOUT INJECTION VS. NON-DIMENSIONAL DISTANCE. Injection at 10% chord, zero incidence angle.

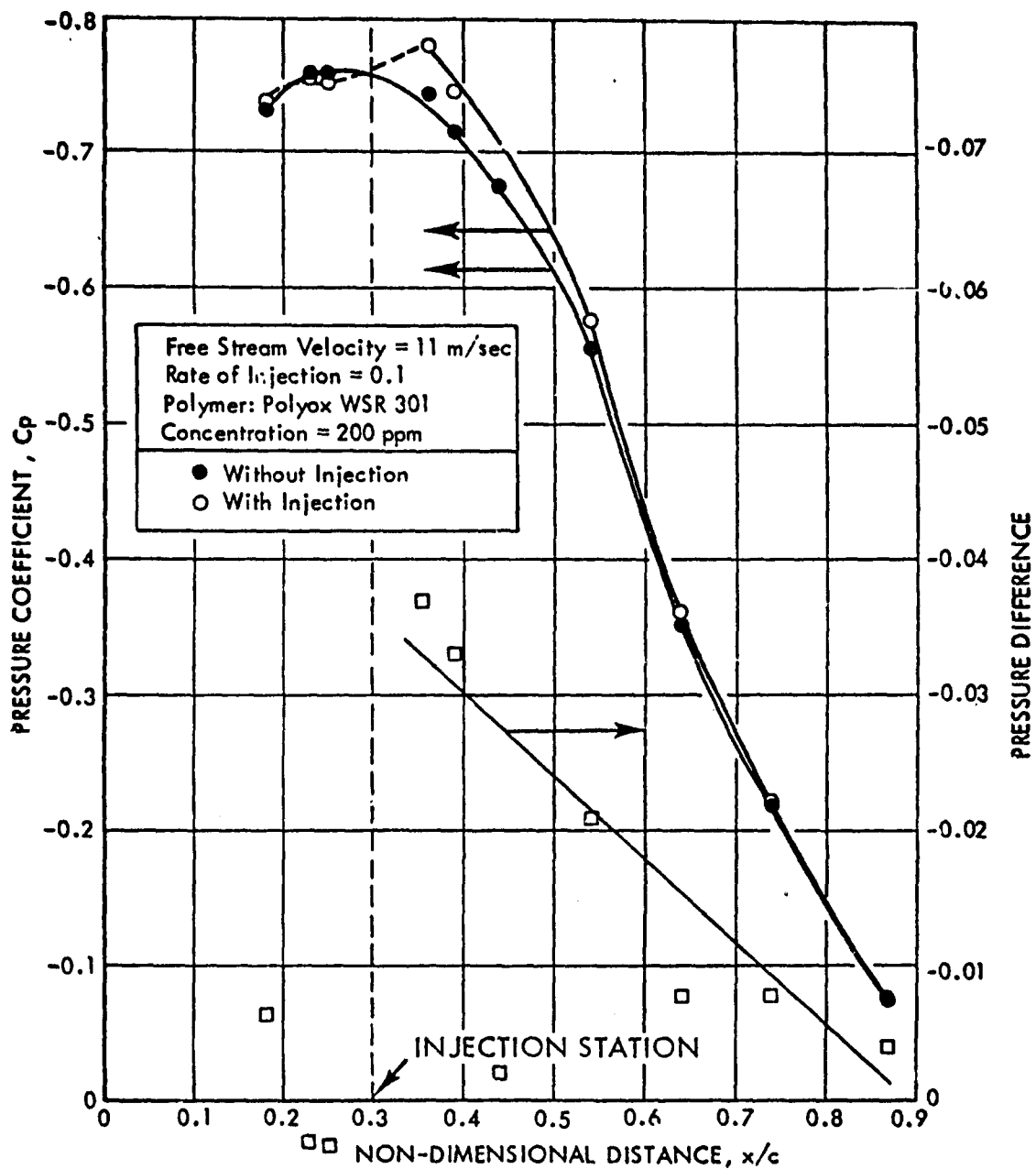


FIGURE 8 - PRESSURE COEFFICIENT WITH AND WITHOUT INJECTION VS. NON-DIMENSIONAL DISTANCE. Injection at 30% chord, zero incidence angle.

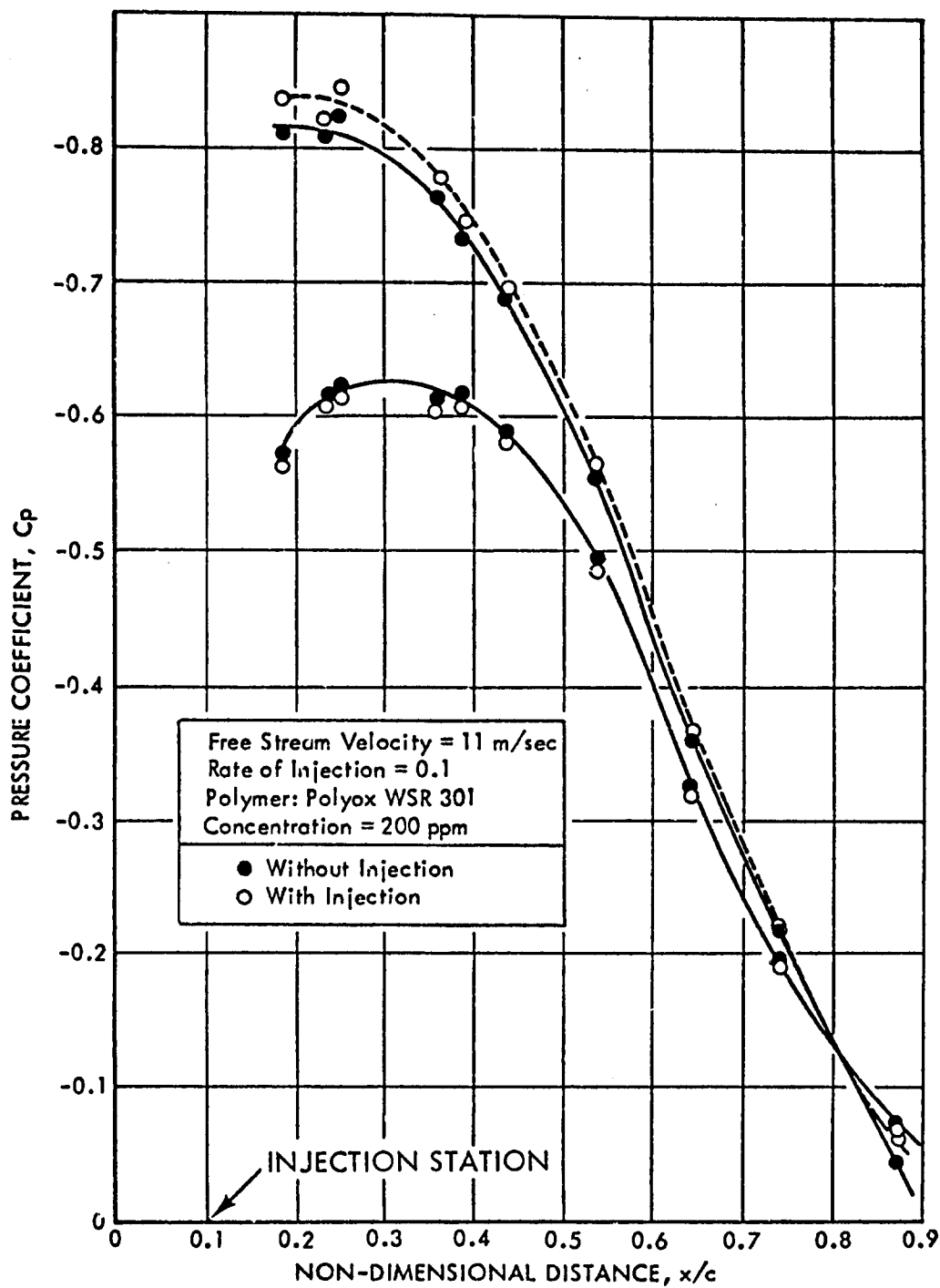


FIGURE 9 - PRESSURE COEFFICIENT VS. NON-DIMENSIONAL DISTANCE ON SUCTION AND PRESSURE SIDE OF HYDROFOIL FOR AN INCIDENCE ANGLE OF $+2.5^\circ$. Injection at 10% chord on the upper surface.

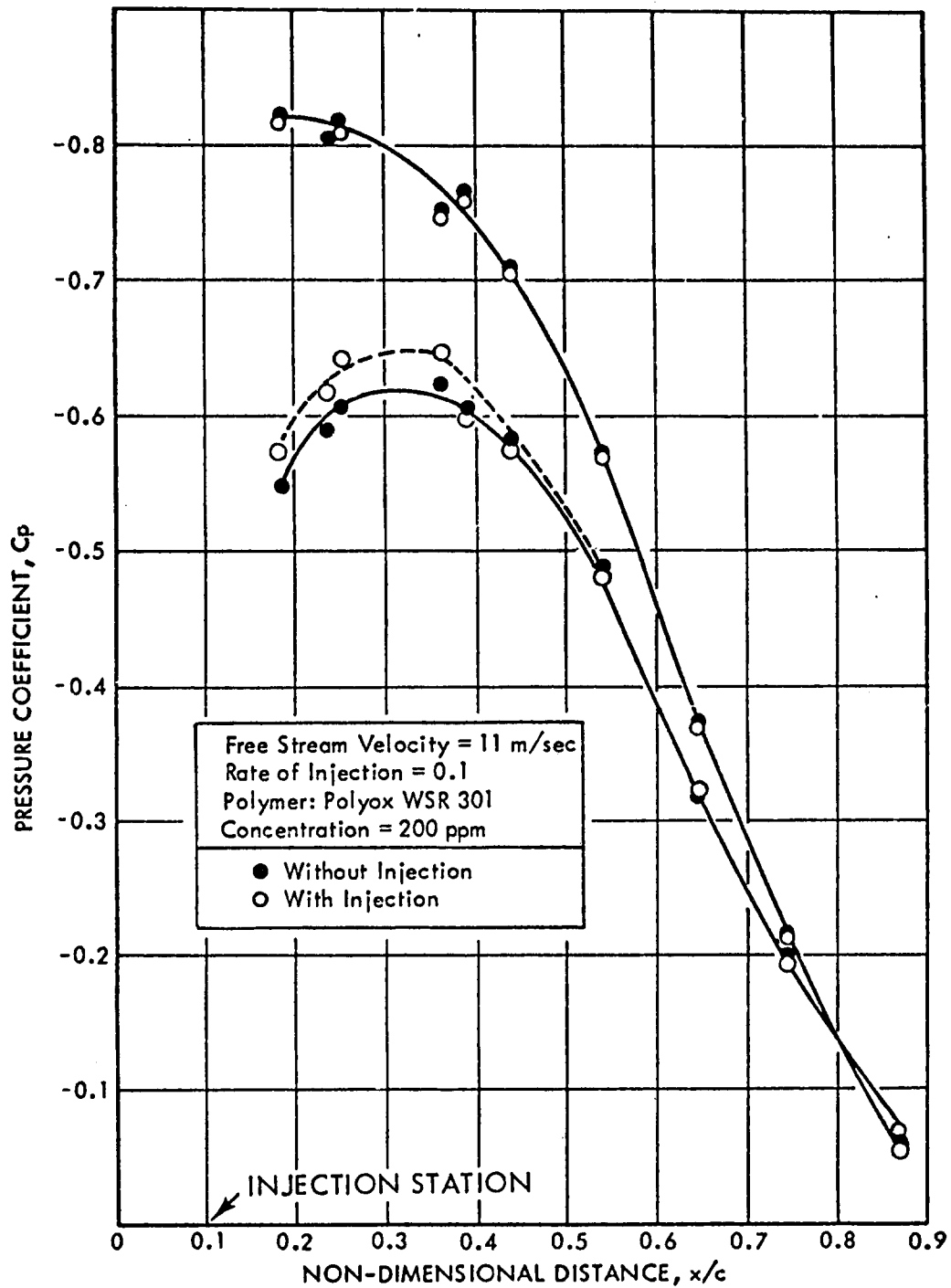


FIGURE 10 - PRESSURE COEFFICIENT VS. NON-DIMENSIONAL DISTANCE ON SUCTION AND PRESSURE SIDE OF HYDROFOIL FOR AN INCIDENCE ANGLE OF -2.5° . Injection at 10% chord on the upper surface.

HYDRONAUTICS, INCORPORATED

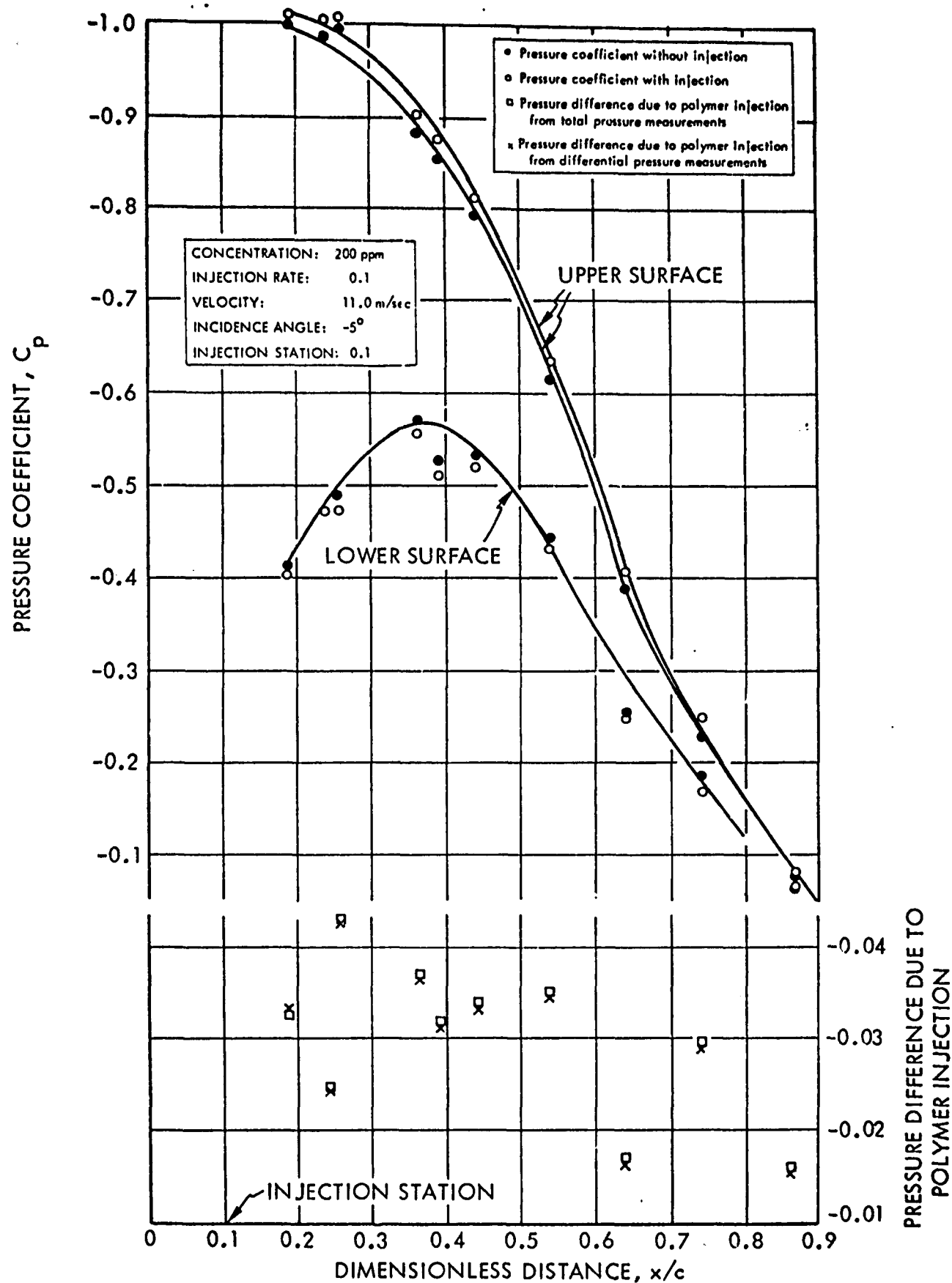


FIGURE 11 - PRESSURE COEFFICIENT VERSUS NON-DIMENSIONAL DISTANCE ON SUCTION AND PRESSURE SIDE OF THE HYDROFOIL FOR AN INCIDENCE ANGLE OF 5° . Injection at 10% chord on the upper surface.

HYDRONAUTICS, INCORPORATED

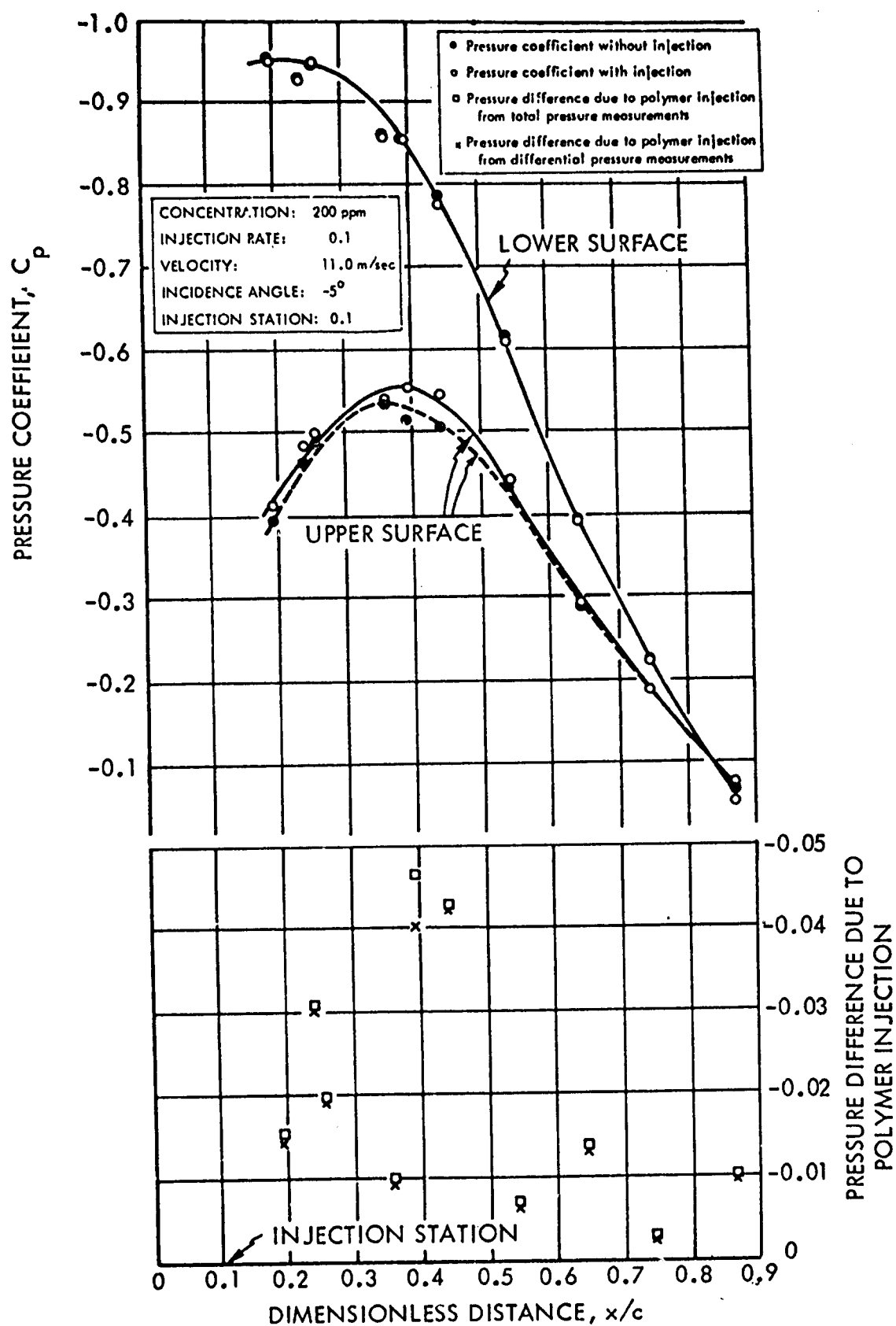


FIGURE 12 - PRESSURE COEFFICIENT VERSUS NON-DIMENSIONAL DISTANCE ON SUCTION AND PRESSURE SIDE OF THE HYDROFOIL FOR AN INCIDENCE ANGLE OF -5° . Injection at 10% chord on the upper surface.

HYDRONAUTICS, INCORPORATED

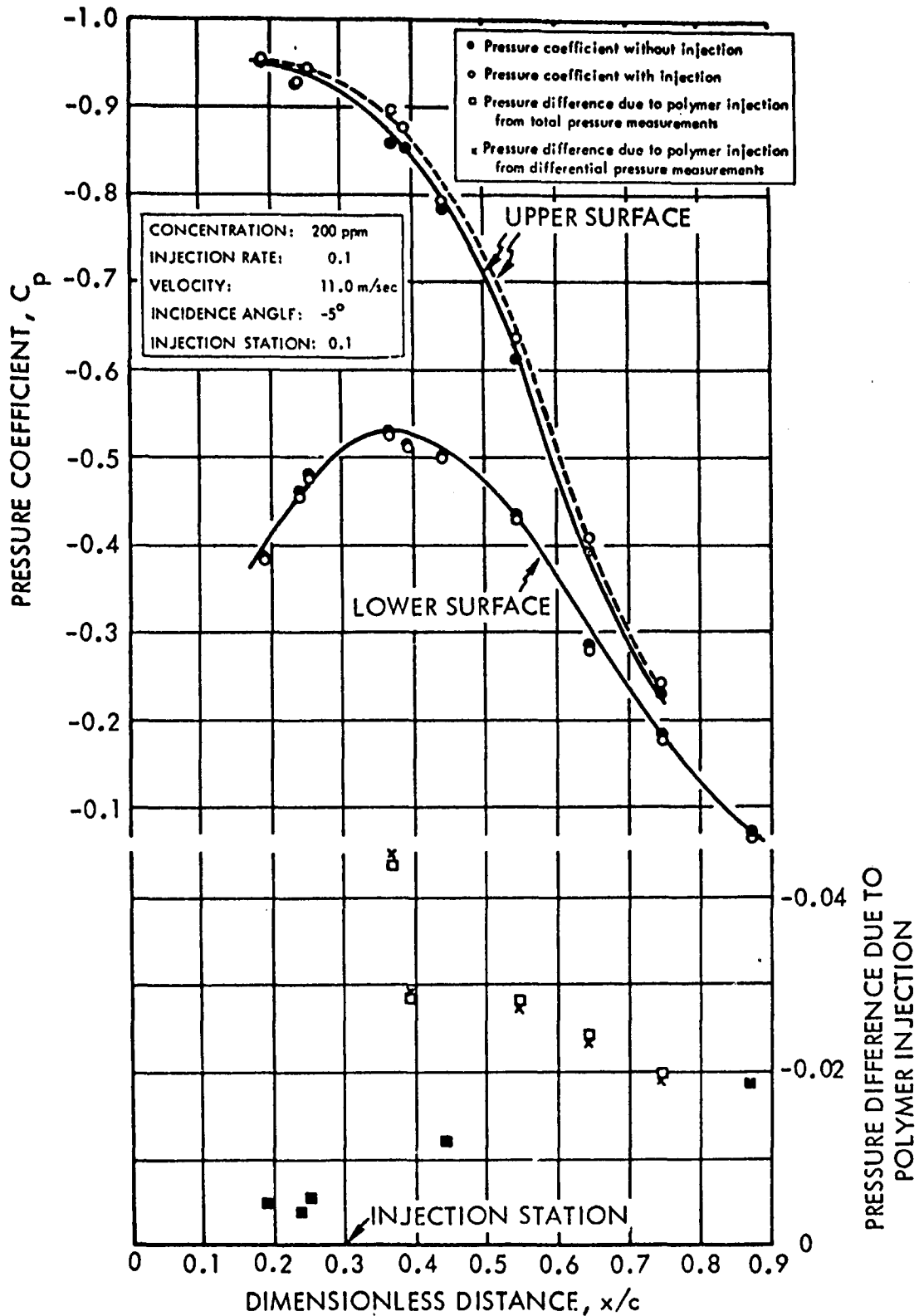


FIGURE 13 - PRESSURE COEFFICIENT VERSUS NON-DIMENSIONAL DISTANCE ON SUCTION AND PRESSURE SIDE OF THE HYDROFOIL FOR AN INCIDENCE ANGLE OF 5° . Injection at 30% chord on the upper surface.

HYDRONAUTICS, INCORPORATED

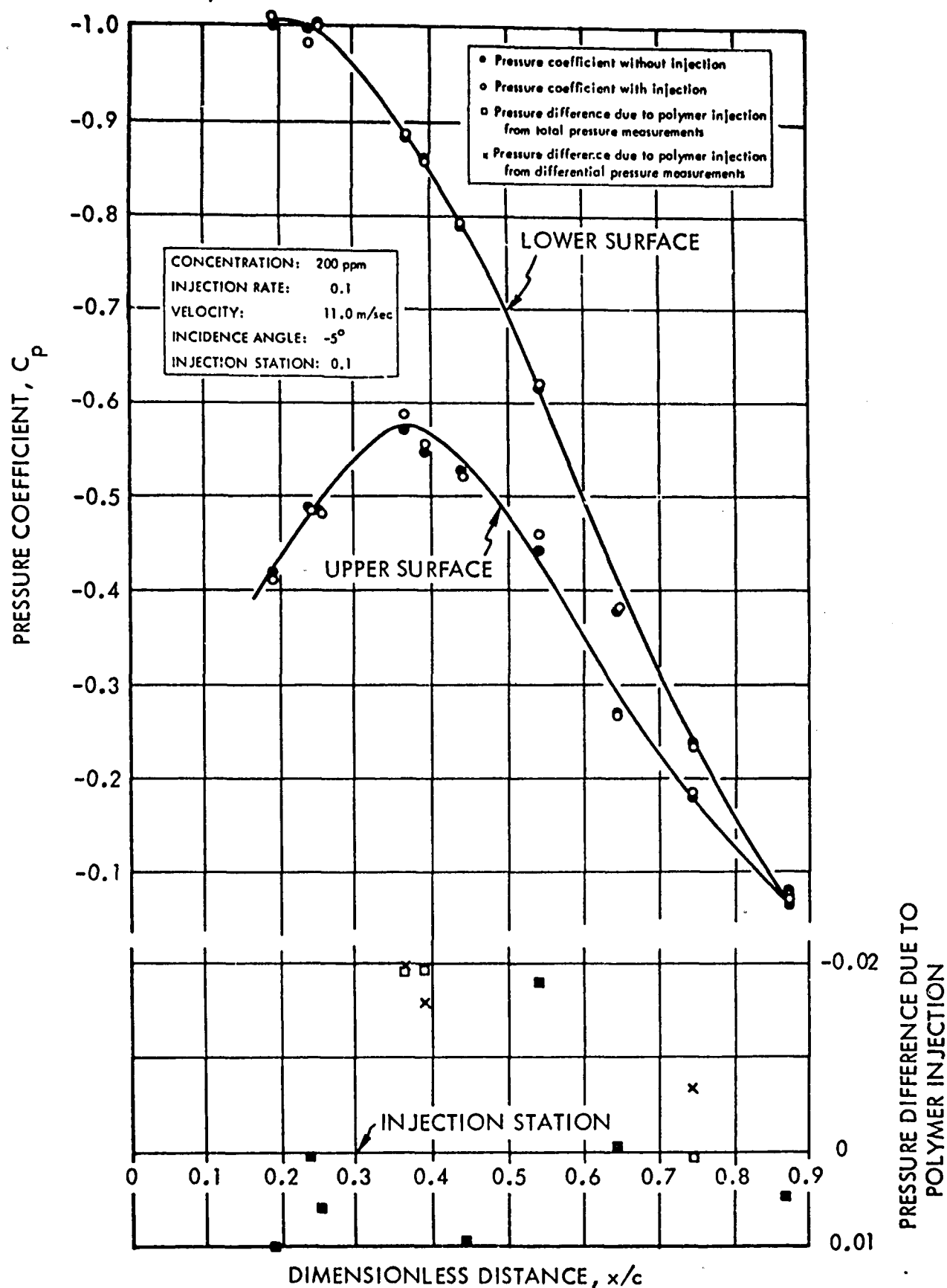


FIGURE 14 - PRESSURE COEFFICIENT VERSUS NON-DIMENSIONAL DISTANCE ON SUCTION AND PRESSURE SIDE OF THE HYDROFOIL FOR AN INCIDENCE ANGLE OF -5° . Injection at 30% chord on the upper surface

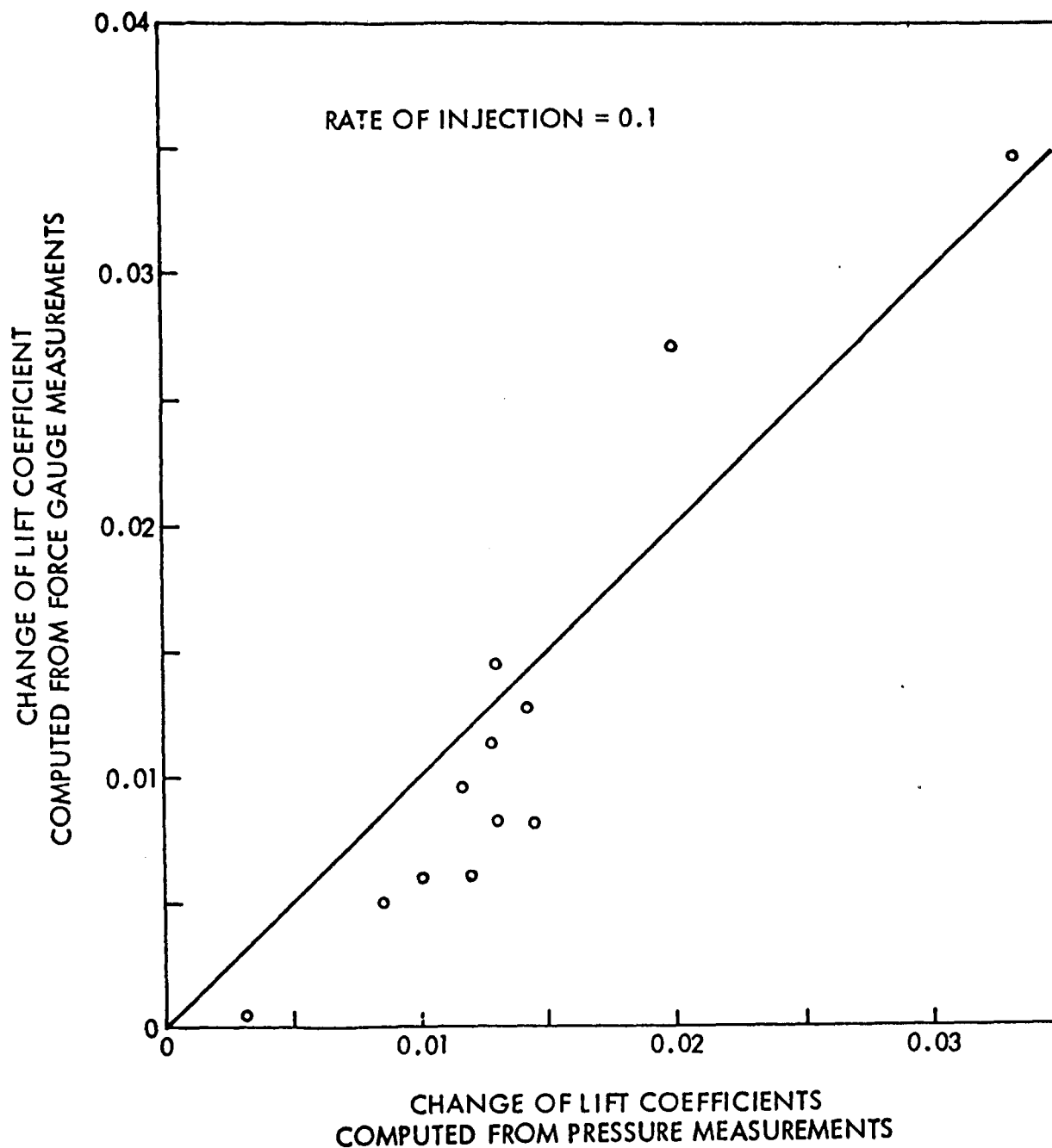


FIGURE 15 - COMPARISON OF THE VALUE OF THE CHANGE OF THE LIFT COEFFICIENT COMPUTED FROM FORCE AND PRESSURE MEASUREMENTS

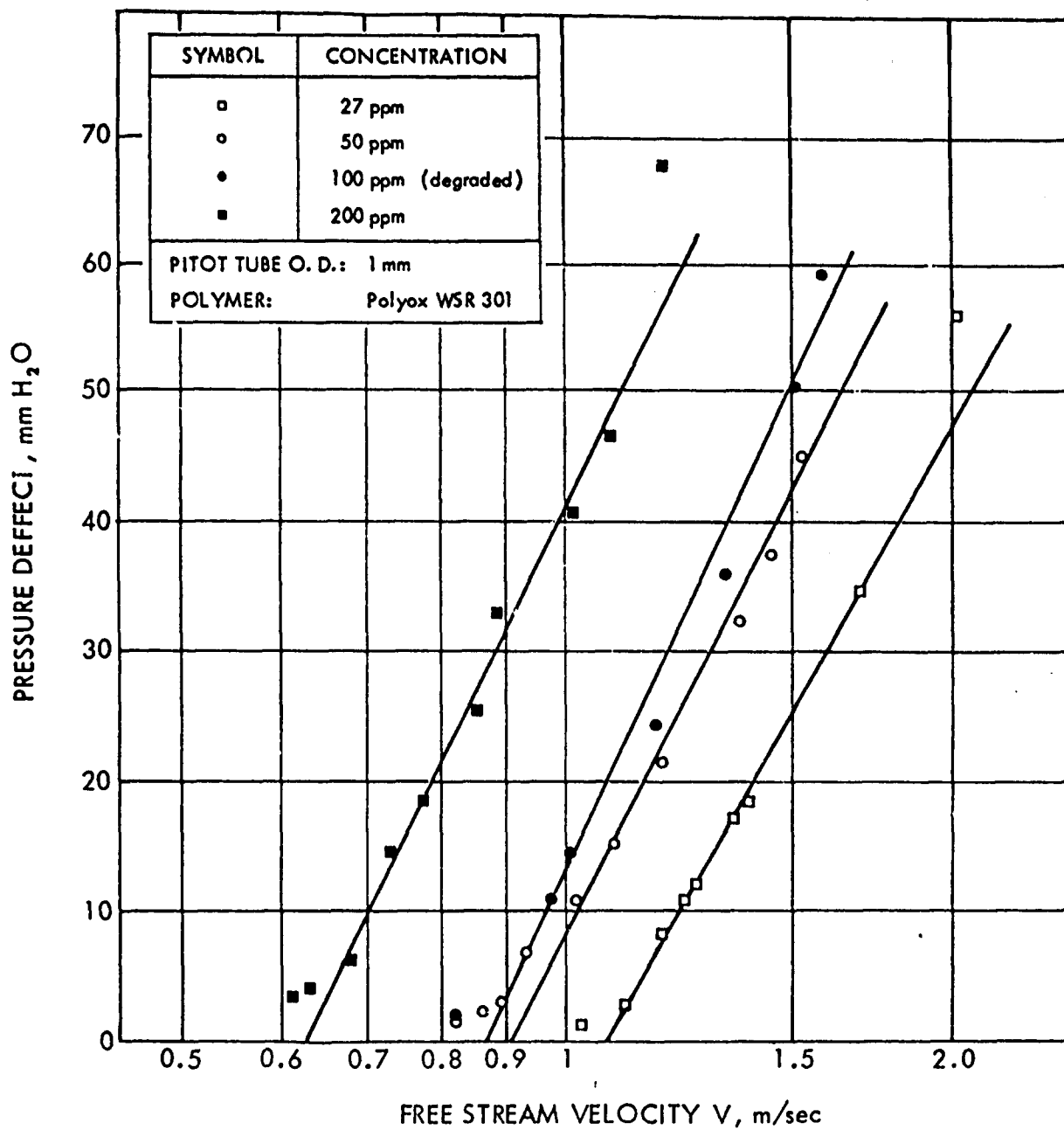


FIGURE 16 - PRESSURE DEFECT MEASUREMENTS WITH A PITOT TUBE PROBE - EFFECT OF POLYMER CONCENTRATION

HYDRONAUTICS, INCORPORATED

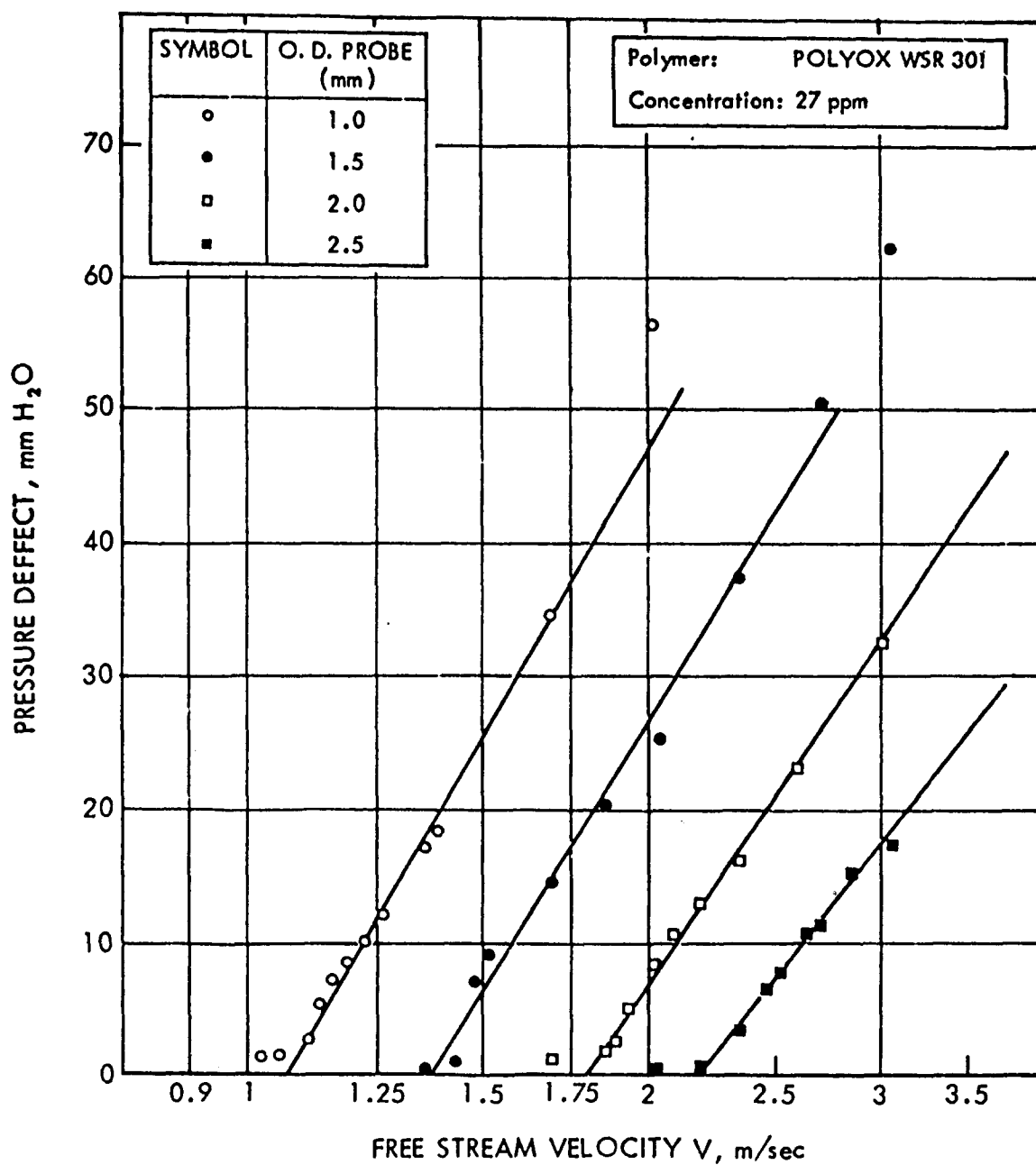


FIGURE 17 - PRESSURE DEFECT MEASUREMENTS WITH A PITOT TUBE PROBE - EFFECT OF OUTSIDE DIAMETER OF PROBE

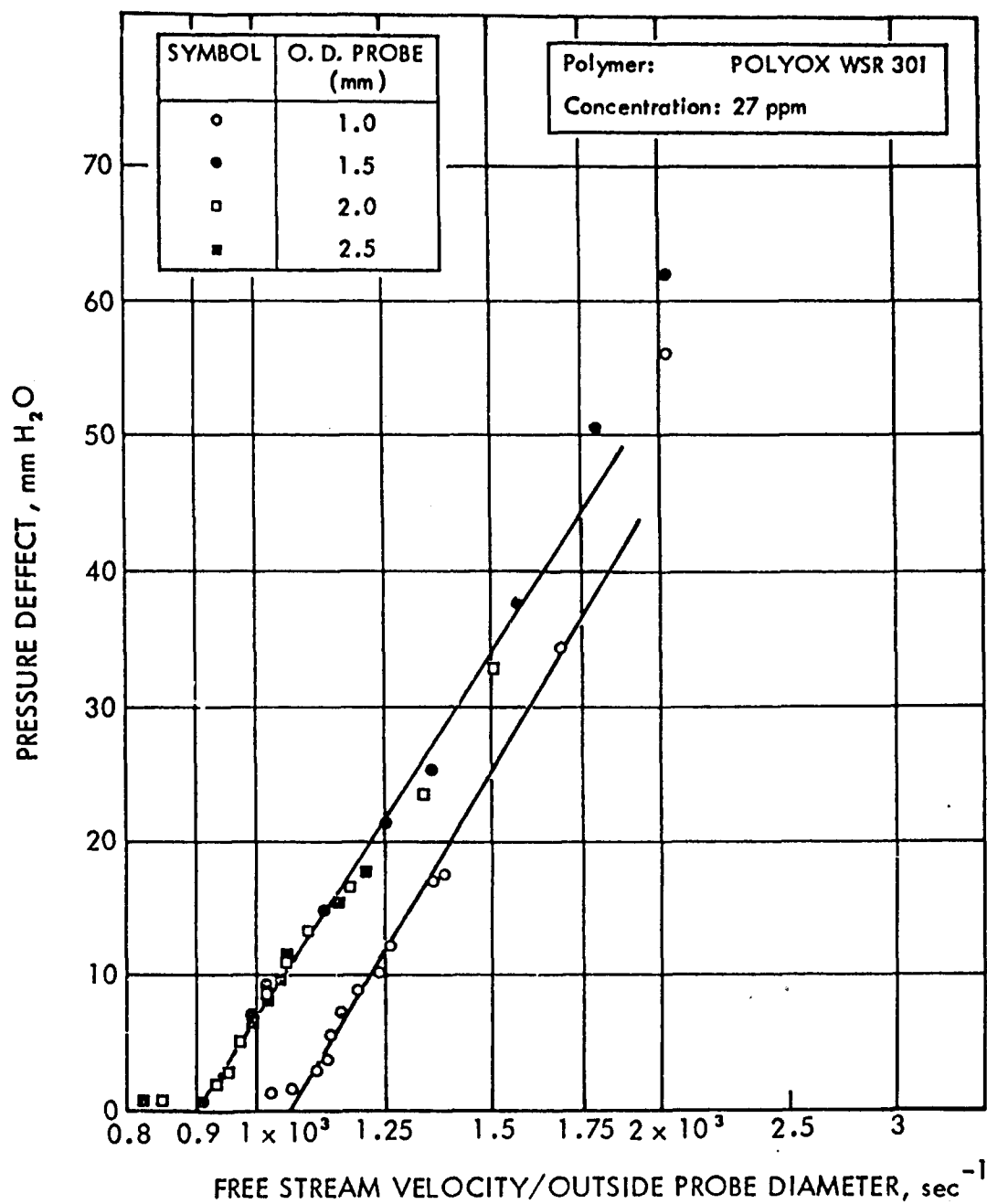


FIGURE 18 - PRESSURE DEFECT MEASUREMENTS WITH A PITOT TUBE PROBE - EFFECT OF VELOCITY OVER OUTSIDE DIAMETER RATIO

HYDRONAUTICS, INCORPORATED

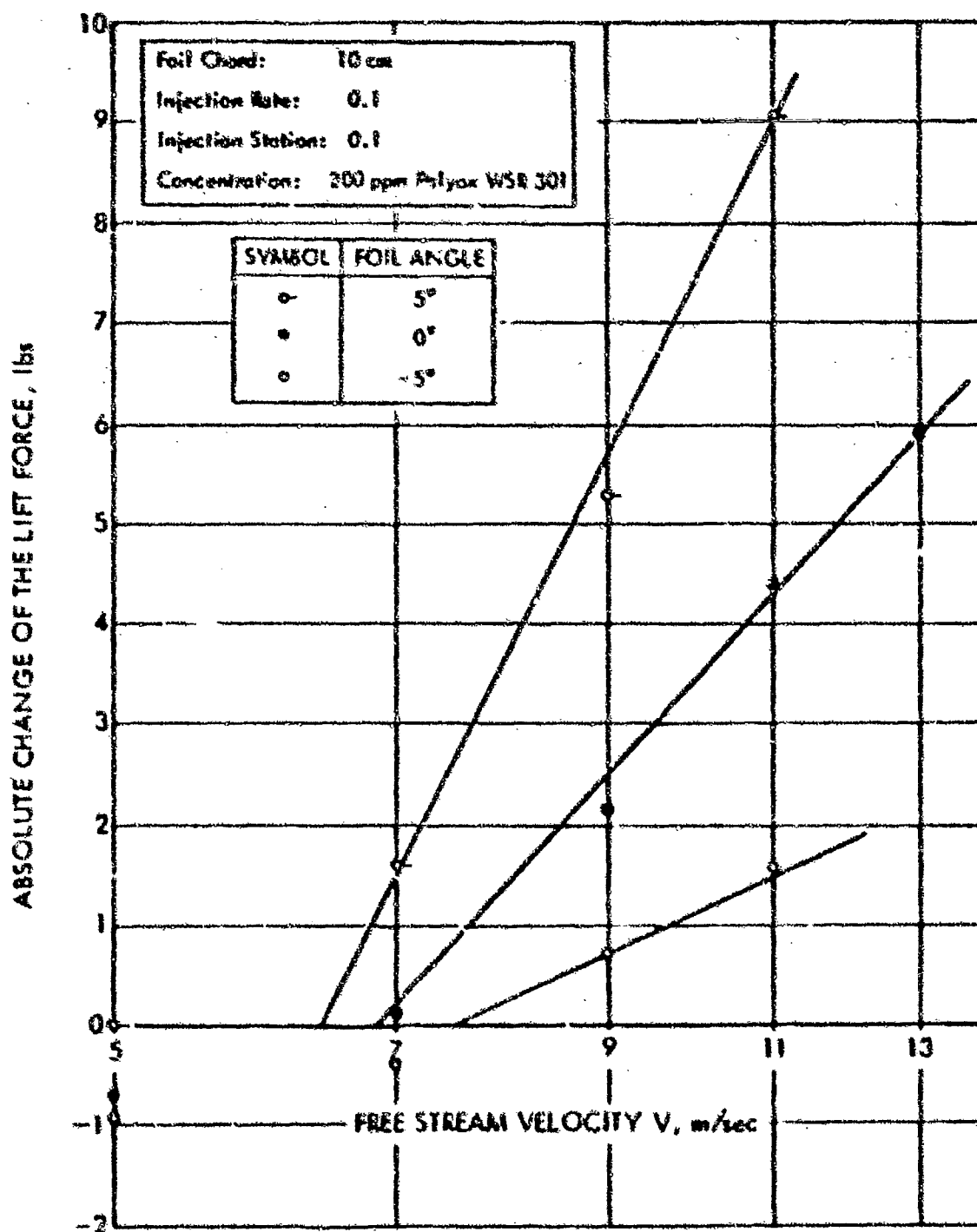


FIGURE 19 - ABSOLUTE CHANGE OF THE LIFT FORCE VERSUS FREE STREAM VELOCITY

HYDRONAUTICS, INCORPORATED

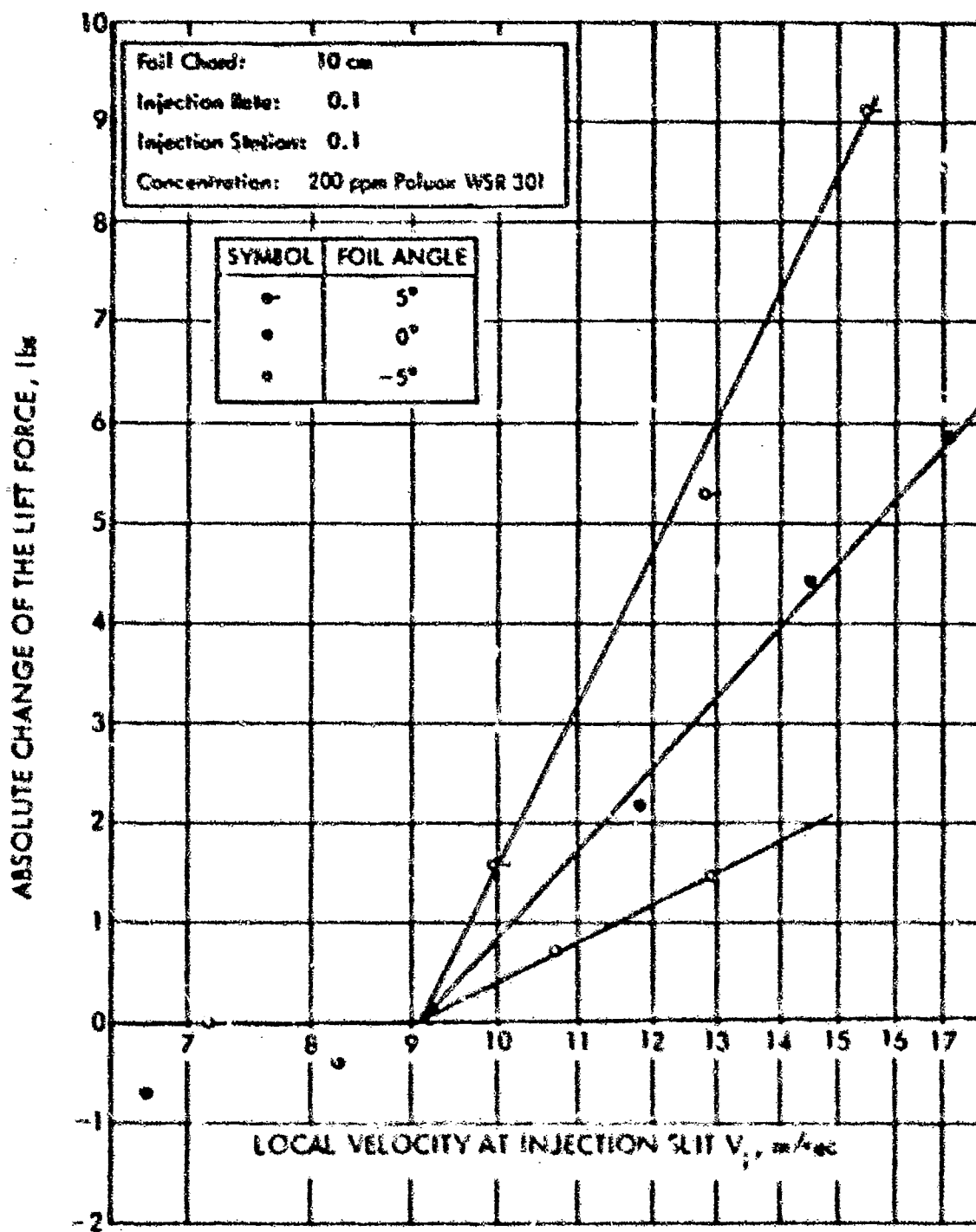


FIGURE 20 - ABSOLUTE CHANGE OF THE LIFT FORCE VERSUS LOCAL VELOCITY AT THE INJECTION STATION

HYDRONAUTICS, INCORPORATED

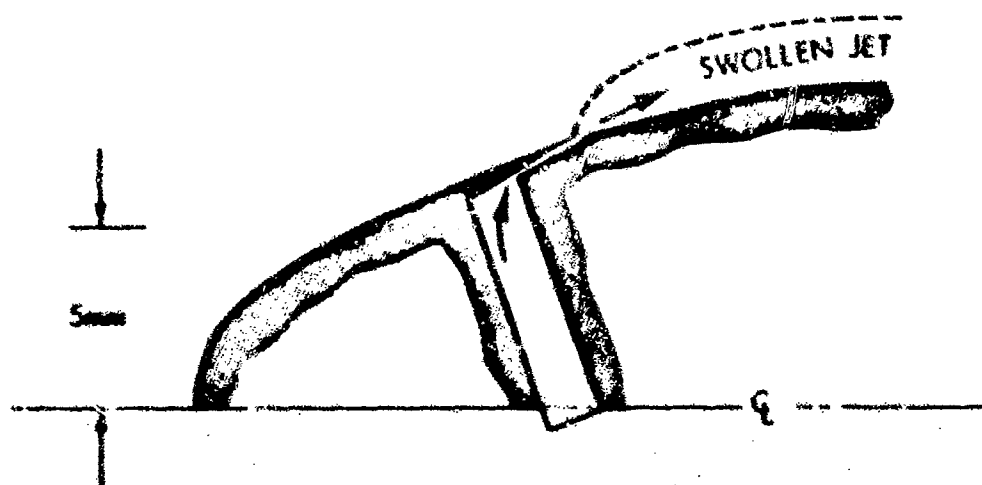


FIGURE 21 - DISTURBANCE DUE TO JET SWELLING